5-2016

ANALYSIS OF TUMOR SPECIFIC PROTEIN EXPRESSION IN GLIOBLASTOMA MULTIFORME (GBMs) TUMORS THROUGH IMMUNOHISTOCHEMISTRY

Amanda M. Wigand
awigand@nmu.edu

ANALYSIS OF TUMOR SPECIFIC PROTEIN EXPRESSION IN GLIOBLASTOMA MULTIFORME (GBMs) TUMORS THROUGH IMMUNOHISTOCHEMISTRY

By

Amanda M. Wigand

Thesis
Submitted to Northern Michigan University
In partial fulfillment of the requirements For the Degree of

MASTERS OF SCIENCE

Office of Graduate Education and Research

May 2016

SIGNATURE APPROVAL FORM

Title of Thesis: ANALYSIS OF TUMOR SPECIFIC PROTEIN EXPRESSION IN GLIOBLASTOMA MULTIFORME (GBMs) TUMORS-THROUGH IMMUNOHISTOCHEMISTRY

This thesis by Amanda Wigand is recommended for approval by the student's Thesis Committee and Department Head in the Department of Biology, and by the Assistant Provost of Graduate Education and Research.

_____

Committee Chair: Robert Belton, PhD Date

_____

First Reader: Robert Winn, PhD Date

_____

Second Reader: Valerie Hedges, PhD Date

_____

Third Reader: Erich Ottem, PhD Date

_____

Department Head: John Rebers, PhD Date

_____

Dr. Robert Winn Date

Interim Assistant Provost of Graduate Education and Research

ABSTRACT

ANALYSIS OF TUMOR SPECIFIC PROTEIN EXPRESSION IN GLIOBLASTOMA MULTIFORME (GBMs) TUMORS-THROUGH IMMUNOHISTOCHEMISTRY

By

Amanda M. Wigand

GBM tumors are the most aggressive and, unfortunately, the most fatal form of brain cancer. GBM tumors with isocitrate dehydrogenase-1 (IDH1) mutation being expressed, lead to higher survival rates in patients that also have full resection of the tumor and chemotherapy. Without this mutation, it is thought that tumors have a higher expression of the protein Basigin and O6-methylguanine-DNA-methyltransferase (MGMT) present, causing it to be more aggressive and less responsive to standard care. The objective of this study was to understand the correlation between IDH1 mutation presence and the expression of Basigin and MGMT. The expression of these proteins was observed in tissues sections from GBM tumors. Proteins were labeled with a fluorescent antibody and imaged with a confocal microscope. The tissue images were then analyzed using Imaris software. It was shown that there was a significant difference between the presence of the IDH1 mutation and Basgin, and also MGMT among all of the tissue blocks.

ACKNOWLEDGEMENTS

The amount of support that I have received since first coming to Northern Michigan University my freshman year until now has been tremendous. I would like to especially thank my undergraduate and graduate advisor, Dr. Robert Belton, for his help with my research and always pushing me to find a solution. This research would not have been possible without my research mentors Dr. John Lawrence, Cathy Bammert, Dr. Erich Ottem, Dr. Robert Winn, Dr. Alan Rebertus, Dr. John Weiss, and Dr. VanGrisven. I would also like to thank the Upper Michigan Brain Tumor Center's intelligent graduate and undergraduate students including Samantha Wightman, Marissa Kane, Chris McMahon, Melanie Flaherty, and Bridget Waas. Most of all I would like to thank my parents and Kevin Burek for their continued support during my time at Northern and throughout life.

TABLE OF CONTENTS

List of Figures v
List of Symbols and Abbreviations vi
Introduction 1
Chapter One: Literature review 3
Cancer development and GBMs 3
Primary vs. secondary GBM 5
Morphology of GBM tumors 7
IDH1 8
MGMT and Temozolomide 9
Basigin 11
Chapter Two: Experimental design 14
Human GBM samples 14
Human GBM cell lines 15
Immunoblotting and antibodies 15
Histochemistry 16
Immunostaining and confocal imaging 17
Statistical analysis 17
Chapter Three: Results 19
Hematoxylin and Eosin Analysis 19
Protein expression within GBM cell lines 19
Protein expression within GBM tissue blocks 20
Analysis of protein expression in GBM samples 21
Chapter Four: Discussion 22
References Cited 67

LIST OF FIGURES

Figure 1: Isocitrate Dehydrogenase (IDH) enzyme function within human cells 26

Figure 2: Common Temozolomide-induced DNA lesions appear on guanine and adenine.....27

Figure 3: Temozolomide is converted to MTIC within the body and contributes methyl or alkyl chemical groups to the purines on DNA.....28

Figure 4: Microvesicles and exosomes are membrane vesicles released from cells to the extracellular space.....29

Figure 5a-e: H&E staining from GBM tumor blocks 30

Figure 6: Immunoblotting of human cell lines with the MGMT antibody 36

Figure 7: Immunoblotting of human cell lines with the Basigin antibody 37

Figure 8: Immunoblotting of human cell lines with the IDH1 antibody 38

Figure 9: Immunoblotting of human cell lines with the IDH1 mutant antibody 39

Figure 10: Immunoblotting of human cell lines with the GAPDH antibody.....40

Figure 11a-e: Immunofluorescence of block 5653 41

Figure 12a-e: Immunofluorescence of block 3331 45

Figure 13a-e: Immunofluorescence of block 4946 50

Figure 14a-e: Immunofluorescence of block 10168 55

Figure 15a-e: Immunofluorescence of block 8072 60

Figure 16a-b: Comparison of immunofluorescence and protein area.....65

LIST OF SYMBOLS AND ABBREVIATIONS

GBM- Glioblastoma Multiforme

IDH- Isocitrate Dehydrogenase

MGMT- O-6-methylguanine-DNA methyltranserfase

DNA- Deoxyribonucleic acid

CNS- Central nervous system

CSC- cancer stem cell

EGFR- Epidermal growth factor receptor

MDM2- Murine Double-Minute 2

VEGF- vascular endothelial growth factor

MVP- microvascular proliferations

AML- acute myelogenous leukemia

ALL- acute lympoblastic leukemia

CIMP- CpG island methylator phenotype

TMZ- Temozolomide

MMP-matrix metalloproteinase

INTRODUCTION

Glioblastoma multiforme (GBM) tumors are the most common and aggressive form of brain tumor in humans[1]. Death from GBM tumors is associated with the rapid rate of tumor growth, which can double in size every two weeks. GBM tumors are classified as either primary or secondary tumors. Primary GBMs generally form in older individuals, and the tumors progress rapidly resulting in the quick onset of symptoms and relatively short patient survival times[2]. These primary tumor types are the most common and deadly form of GBMs. Secondary GBMs generally occur in people at age forty-five or younger and represent ten percent of all GBMs[3]. Secondary GBMs tend to grow at a slower rate and are more responsive to treatment, however they are, none-the-less, deadly if not treated. GBM tumors appear heterogeneous in their composition, as they will contain several different substances, including cystic minerals, calcium deposits, blood vessels, and dead cells. Because of their location within the brain, GBMs rarely metastasize to other regions of the body. However, presence of tumor tissue within the brain results in significant morbidity as the tumor invades and crowds out normal brain tissue [2].

The ability to distinguish between GBM tumors of differing severity is central to the efforts to develop novel therapies. For example, many GBM tumors over-express DNA repair enzymes like O-6-methylguanine-DNA methyltransferase (MGMT), which makes them resistant to chemotherapy and radiotherapy treatments [4]. MGMT does not play a role in tumor development, it is mainly utilized for tumor

maintenance. Identifying proteins associated with resistant GBM tumors is a necessary first step in the process of developing novel therapies. Currently, our work is focused upon three specific proteins known individually to play a significant role in the development of GBM tumors: Basigin, MGMT, and IDH1.

CHAPTER ONE: LITERATURE REVIEW

Cancer Development and GBMs

The development of cancer in humans can occur in response to many different kinds of damage to DNA, including exposure to toxic substances, viruses, or radiation. In all cases, the main hallmark of cancer development is the abnormal proliferation of cells collectively, referred to as neoplasia. Tumors develop from normal cells in stages as the cancer develops an ever-increasing ability to proliferate. Thus, the terms hyperplasia, metaplasia, and dysplasia have been used to describe the increasing proliferative capacity, with dysplastic tumors being the most aggressive cancers[5]. Hyperplasia refers to tissues that appear normal but are growing inappropriately. Metaplasia refers to tissues that are still exhibiting functional characteristics, but demonstrate the overgrowth of one tissue or cell type over another. Lastly, cells or tissues that appear abnormal and are clearly growing in an uncontrolled fashion are referred to as dysplastic[5]. The multiple-hit hypothesis for tumor formation (also called the Knudson hypothesis) states that dysplastic tumors contain cells with two or more mutations to important growth regulatory genes[6]. For example, a mutation that inactivates a gene that normally suppresses cell growth (tumor suppressor genes) can result in a cell growing and dividing uncontrollably[6]. Such tumor suppressor genes act as brakes to prevent abnormal cell growth. Conversely, mutations that activate normally inactive genes or amplify genes that are not regularly transcribed, resulting in cell proliferation, are referred to as proto-oncogenes. In this case, mutations to proto-oncogenes can convert them to oncogenes resulting in the production of proteins that

are constitutively active and promote cell proliferation. The Knudson hypothesis proposes that cells generally require both the inactivation of tumor suppressor genes and the activation of proto-oncogenes to form dysplastic tumors[5].

Within GBM tumors exists a population of cells that play a central role in tumor progression. These so-called cancer stem cells (CSCs) are slow growing and possess properties of stem cells, including the ability for self-renewal. Like other stem cells, CSC appear to be resistant to chemotherapeutics, possess an enhanced ability to repair damage to DNA, and are able to regenerate tumors following surgical removal of the original tumor [7]. Furthermore, CSC are able to divide without differentiating and thus can provide a reservoir for the formation of new tumors [8]. It is unknown whether the CSCs are the cancer initiating cells of a GBM tumor, or whether they represent a population of dysplastic cells that have de-differentiated to form stem cell-like cells.

It is widely accepted that brain tumors can arise from a number of different glial cell types such as, glial progenitor cells, astrocytes, or oligodendrocytes, giving rise to tumors of varying severity[9]. GBMs that arise from glia or other precursor cells within the central nervous system (CNS) cause their specific pathologies as the tumors proliferate in an uncontrolled fashion. A number of changes have been identified in GBM tumors, including either an insensitivity or oversensitivity to cell autonomous signals, or self-signaling, hypermethylation or hypomethylation of chromatin regions surrounding key cellular growth or apoptosis genes, and specific mutations within the DNA[10]. A particularly significant mutation found within GBMs and lower grade gliomas occurs to the Isocitrate dehydrogenase 1 gene (IDH1). Point mutations to the IDH1 gene can produce an arginine-to-histidine amino acid change at amino acid 132 of the IDH1

enzyme (called the IDH1 R132H mutant).This mutation leads to sensitivity to reactive oxidative species. Reactive oxidative species are a collection of molecules produced by normal cellular metabolism that can cause cellular damage. In its normal state, it has been shown that IDH1 may function to help maintain the redox state within the cell and promote cellular defense against oxidative damage[11]. The point mutation to IDH resulting in IDH1 R132H produces an oncogene that has a role in oncogenesis and may be an important possibility for therapeutic interventions[10].

GBM tumors tend to experience changes in the expression profiles for many genes which confers a phenotype that resists treatment and promotes cancer growth; the enzyme O-6-methylguanine-DNA methyltransferase (MGMT) falls in this category. MGMT is a DNA repair enzyme that removes chemical adducts from damaged DNA, preventing future damage, specifically from the O6 guanine residue[12]. The chemotherapeutic drug Temozolomide (TMZ), which is the standard chemotherapy agent used to treat GBM tumors, functions by adding alkyl or methyl groups to the N7 position of guanine, N3 position of adenine, and the O6 guanine residues[4]. TMZ induces DNA damage, most importantly to the O6 guanine residue, the most cytotoxic location, stimulating apoptotic processes that result in the death of the rapidly growing cells found within the tumor. However, when a tumor cell overexpresses the MGMT enzyme, such cancers can evolve resistance to alkylating therapeutic agents like TMZ[13]. Therefore, a comprehensive understanding of the expression patterns for DNA repair enzymes, such as MGMT, in patient tumors, is central in our efforts to effectively treat GBM patients [4].

Primary vs. Secondary GBM

Primary and secondary tumors are thought to arise from different populations

and are characterized by different genetic changes within each [9]. More importantly, primary tumors tend to be more aggressive and arise in older populations, while secondary tumors are less aggressive and occur in younger populations[14]. Primary tumors often have genetic alterations including the loss of the proximal arm of chromosome 10 (called LOH 10p), amplification of epidermal growth factor receptor gene (EGFR) and Murine Double Minute-2 oncoprotein (MDM2) gene, and inactivating mutations to the PTEN tumor suppressor gene[14]. Primary tumors also develop rapidly after a short clinical history and with very little evidence of less malignant preceding tumors[15]. Consequently, these tumors are extremely aggressive in their growth and resistance to treatment, and result in a poor prognosis for patients[14].

Secondary GBMs area characterized by a loss of the distal arm of chromosomes 19 and 22 (19q, 22q), and mutations in the TP53 tumor suppressor gene. Secondary GBMs are more likely to develop from slow growing and well-differentiated low-grade astrocytomas. These tumors have a tendency to slowly invade other brain tissues, develop into an anaplastic astrocytomas, and eventually form secondary GBMs[15]. The TP53 mutation is considered an early mutation in the sequence of tumor formation, as it occurs in low-grade, diffuse astrocytomas as well as in most secondary GBMs[14]. TP53 is commonly mutated in a number of different human cancer types as the p53 protein, which is produced as a product of the TP53 gene, is a master regulator of the cell cycle and is important for the suppression of tumor development. Inactivating mutations to TP53 generally involve a single base substitution, and subsequent loss of the remaining wild type allele[16]. TP53 mutations are known to be very diverse in their sequence context, position and structure, and generally result in a missense mutation causing a

single amino-acid change in the p53 protein[16]. Interestingly, TP53 mutations and IDH1 mutations are generally both present within secondary GBMs [3].

Morphological Characteristics of GBM tumors

GBM tumor tissue is heterogeneous in nature and can vary widely in both the cellular and vascular forms. Analysis of tumor architecture is performed by histochemical analysis of biopsied tissues. Histological analysis of tumors is the gold standard utilized by pathologists to assess the 'tumor grade' of a patient. According the World Health Organization (WHO), a grade IV astrocytoma is classified as a GBM and will generally contain a variety of cell types, microvascular proliferation (MVP), endothelial hyperplasia and hypertrophy, glomeruloid vessels and cellular necrosis[17]. MVP is the formation of a new blood supply to the tumor and has been causally linked to other significant characteristics of GBMs, including hypoxia-induced gene expression changes and the expression of cytokines such as vascular endothelial growth factor (VEGF)[17]. MVP is linked to the appearance of necrosis within the tissue. All of these morphological conditions can be visualized using histochemical techniques to more accurately predict overall survival of a patient[17]. However, histochemical analysis is limiting because it does not provide information regarding the expression of particular oncogenes or tumor suppressors within the tumor. Because of the heterogeneity of cells in GBM tumors, the identification of particular cell types, oncogenes, and tumor suppressor proteins is critical for effective therapeutic approaches. Such an approach, if available, would give health care providers critically important information regarding tumor treatment and possibly improve patient outcomes. To this end, we propose to utilize immunohistochemical analysis of human tumors and attempt to correlate the known severity of human GBM tumors with the

expression of three cancer cell markers: IDH1-R132H, MGMT, and Basigin.

IDH1

The human genome possesses five IDH genes that give rise to different isozymes of the IDH protein, including IDH1, IDH2, IDH3A, IDH3B and IDH3G[18]. In cells, the IDH1 and IDH2 proteins both function as homodimers by binding with an identical protein subunit to initiate catalytic activity. The three IDH3 isozymes form dimers composed of either two alpha subunits, or one beta and one gamma subunit. IDH proteins function within both the cytosol (IDH1) and mitochondria (IDH2 and IDH3) to generate reduced nicotinamide adenine dinucleotide phosphate, NADPH, from $NADPH^{+}$[18]. IDH1 to catalyze the oxidative decarboxylation of isocitrate to alpha-ketoglutarate (α-kg) [11]. IDH2 and IDH3 proteins function within the mitochondria in the Kreb cycle by converting isocitrate to α-KG and reducing Nicotinamide adenine dinucleotide NAD+ to NADH[11]. The Kreb cycle is utilized by cells to generate adenosine triphosphate molecules through different enzymatic reactions.

The most common IDH mutation found in GBMs is an IDH1 point mutation that converts the arginine residue at position 132 to histidine, called IDH1 R132H [19]. This IDH1 mutation is also found in other cancers including acute myelogenous leukemia (AML), cholangiocarcinoma, cartilaginous tumors, prostate cancer, papillary breast carcinoma, acute lympoblastic leukemia (ALL), angioimmunoblastic T-cell lymphoma, and primary myelofibrosis[11]. IDH1 R132H mutations are present within 55% to 80% of grade II and III gliomas and are commonly present within secondary GBMs. GBM patients that carry the IDH1 R132H mutation experience improved survival following maximal resection of the tumor [20]. Thus, knowledge of the mutation status for IDH1 in

brain cancers can lead to a better prognosis for patients. The effect of the R132H mutation is the production of the oncometabolite 2-hydroxyglutarate (2-HG; see also figure 1) [21].

The production of 2-HG induces changes in DNA methylation pathways and gene expression in cell, ultimately, promoting tumorigensis. Known as the CpG island methylator phenotype (CIMP), 2-HG induced DNA methylation is an indirect result of the IDH R132H mutation. CIMP is correlated with widespread hypermethylation in genes at specific loci [22]. It is currently unclear how the IDH1 mutation initiates tumor growth and lead to CIMP in any type of cancer [21]. Even though mutant IDH1 is viewed as an oncogene, information about its presence within a tumor can be helpful as patients treated with Telozolomide (TMZ) and radiation can experience greatly improved survival times[23].

MGMT and Temozolomide

MGMT is an enzyme that removes chemical adducts from DNA, thus preventing damage to the DNA. This DNA repair enzyme, when present in tumors, can reverse the DNA damaging effects of chemotherapeutics such as TMZ [12]. Thus, increased levels of the MGMT enzyme correlate with poor responses to TMZ. Most cells express MGMT enzymes, and the expression of the MGMT gene can be induced by DNA damage [24]. Interestingly, some cells will exhibit greatly reduced levels of the MGMT protein as a result of MGMT promoter methylation events[25]. In such cells, the reduction of MGMT enzyme levels allows for TMZ-induced DNA damage and subsequently apoptotic cell death. The expression level of MGMT effects the size of tumors. MGMT promoter methylation and reduced MGMT protein tend to be smaller in size and respond more positively to treatment. In contrast, when the MGMT promoter is not methylated tumors

are larger due to the lack of damage to cellular DNA[26].

As mentioned previously, the primary chemotherapeutic agent utilized to treat GBM tumors is TMZ. TMZ induces the alkylation or methylation of DNA at the N7 position of guanine, N3 position of adenine, and the O6 position of guanine. When the O6 guanine residue becomes methylated it constitutes nearly all of the activity of TMZ but is only five percent of the total adducts added to the DNA. The methylation of guanine causes a mismatch pairing with guanine and tyrosine, triggering apoptotic death of rapidly growing cells such as GBM tumor cells (Figure 2)[4]. The introduction of TMZ in 2007 for GBM patients resulted in the greatest improvement in patient survival ever observed for this deadly cancer [12]. Unlike most chemotherapeutics, TMZ is readily absorbed through oral administration and can easily cross the blood brain barrier. Within the body, TMZ is converted to the active compound 5-(3-dimethyl-1-triazenyl) imidazole-4-carboxamide (MITIC), and the conversion of TMZ to MITIC is pH dependent (Figure 3) [25]. MITIC's main sites of methylation are the N7 position of guanine, the N3 position of adenine and the O6 position of guanine[4]. Cell cycle checkpoint regulators recognize this damage to the DNA and halt the cell cycle. However, the overexpression of MGMT enzymes can reduce the effectiveness of TMZ's effects as the MGMT enzymes repair DNA modifications produced by TMZ [27]. Therefore, information regarding the expression level of MGMT in tumors is central to predicting the effectiveness of TMZ treatment. DNA sequencing of tumor genomes has revealed that MGMT promoter cytosine methylation levels can predict responses to TMZ treatment. Non-methylated MGMT promoter results in elevated expression of the MGMT gene, and thus a reduced responsiveness to TMZ [24]. Therefore, developing

methodologies to identify tumors that express elevated levels of MGMT is central to determining the potential effectiveness of TMZ treatment. Progression free survival (PFS) and overall survival (OS) have been shown to be superior with MGMT promoter methylation and standard care [23].

Basigin

Basigin is a transmembrane glycoprotein with many different cellular functions. Known by many different acronyms, including EMMPRIN and CD147, Basigin is involved in processes such as sexual reproduction, neural function, inflammation, and tumor invasion[28]. Tumors with increased Basigin expression correlate positively with an aggressive invasive phenotype [28]. Elevated Basigin expression in tumors stimulates surrounding tissues to express vascular endothelial growth factor (VEGF), which promotes neoangiogenesis, or the formation and growth of new blood vessels [29]. Additional evidence demonstrates that elevated Basigin stimulates the expression of matrix metalloproteinase (MMP) enzymes needed for remodeling of the extracellular matrix of the tissue surrounding the tumor [30]. Basigin protein functions in a paracrine manner to stimulate surrounding tissues to produce other molecules needed by the tumor to grow and spread. Thus, stimulating other cells to remodel the extracellular matrix and surrounding tissue.

It may seem counterintuitive that a transmembrane glycoprotein can function as a paracrine signaling molecule, but it is well established that Basigin can be released from the surface of tumor cells via microvesicle shedding (Figure 4). In fact, there has been an explosion of data demonstrating that most cells release some form of microvesicle (either membrane microvesicles or exosomes) that can stimulate

surrounding tissues to alter their activity [31]. The release of microvesicles from tumors containing Basigin protein elevates the expression of metalloproteinase enzymes in surrounding cells and promotes remodeling of the extracellular matrix to allow for tumor growth and spread[32]. This phenomenon suggested that there must be a basigin receptor on cells, and Belton et. al., showed that the cell surface Basigin protein was shown to function as a receptor for soluble Basigin protein [33]. In response to soluble Basigin, normal (non-cancerous) cells are stimulated via the p42/44 Map Kinase signaling pathway resulting in elevated expression and secretion of a number of MMP gene products. Therefore, aggressive cancers that express and release greater amounts of Basigin protein are able drive surrounding tissues to synthesize molecules that promote tumor survival. Finally, increased Basigin expression within tumor cells promotes the ability of cancer cells to survive chemotherapy directly. This appears to be a direct result of Basigin's interaction with P-glycoprotein and ATP-binding casset transporters, or ABCG transporters that function to remove toxic compounds from cells and thus assist cell survival pathways in the presence of chemotherapeutic agents[34].

Normal human brain tissue expresses little to no Basigin protein, while brain tumors express elevated levels of Basigin[34]. Furthermore, patients with GBM tumors tend to struggle more with daily activities and general cognitive function when their cancer has higher Basigin levels. This evidence also correlates with reduced overall survival of patients and suggests that Basigin is a critical marker for tumor severity and patient outcomes [34]. Based upon this evidence, we hypothesized that the severity of a particular GBM tumor correlates positively with the expression levels of Basigin and the DNA repair enzyme MGMT, and inversely with the expression of the IDH1 R132H mutant metabolic enzyme. To test this hypothesis, human brain tissues from

GBM patients were analyzed for protein expression using immunohistological staining techniques. The data was collected by confocal microscopy, and quantitatively analyzed using Imaris imaging software.

CHAPTER TWO: EXPERIMENTAL DESIGN

Introduction

While Basigin, MGMT, and IDH1 are all expressed in GBMs, it is not yet known how the levels of expression for each protein affect tumor aggressiveness and resistance to treatment. For this project, commercially available antibodies specific for the target proteins were utilized to identify relative expression levels for each in human tumor samples. GBM cell lines were used to demonstrate that the antibodies specifically recognize their target proteins using a standard immunoblotting approach. Paraffin embedded tumor samples were prepared for fluorescent immunohistochemistry and confocal microscopy to analyze the level of expression. It was expected that increased expression of Basigin and MGMT would correlate with more aggressive GBM tumors. While the IDH1 R132H mutation is not always present within primary GBMs (it is often seen within secondary GBMs), the presence of this mutation would benefit patient survival if the tumor were fully resected and treated with TMZ and radiation.

Human GBM samples

Glioblastoma samples were provided by the UP Health System- Marquette (UPHSM). The use of these tissues was approved by UPHSM Institutional Review Board (IRB) and the Northern Michigan University IRB. The preserved tissue was collected between 2003 and 2004, and patient information associated with the tumor samples was expunged from the records prior to use. The initial histological analysis of the tissues was performed in the Department of Pathology of UPHSM by Dr. John

Weiss. Dr. Weiss provided marking of malignant spots of Hematoxylin & Eosin (H&E) stained tissue sections.

Human GBM Cell Lines

U87MG IDH1 R132H mutant cell line was a kind gift from Horacio Soto at Geffen Cancer Center at UCLA. The U87MG, LN229, T98 (American Tissue Culture Collection Manassas, VA), and fibroblast cell line, MSU 1.1 from Michigan State University. Cell lines were grown in standard conditions of 37°C and 5% CO2 in complete media, Eagle's minimal essential medium and Dulbecco's Modified Eagle's Medium (Lonza, Walkersville, MD) with 10% bovine serum (FBS) (Atlanta Biological, Atlanta, GA) and 1% Penicillin/Streptomycin/Amphotericin B (Gibco, CA) to 80% confluency in T-75 flasks. Cells were harvested using the trypsin-EDTA method (Versene, Lonza) and cells pelleted at 300x g. Cell pellets were washed and resuspended in growth media for replating in tissue cultureware at a ratio of 1/3.

Immunoblotting and Antibodies

Nearly confluent cell monolayers were washed with cold PBS and the cells lysed using a 1% NP-40 non-denaturing detergent buffer. Lysates were clarified by centrifugation (20,000xG, 10 minutes, 4°C) and the supernatant collected. Total protein concentration was determined using the bicinchoninic acid assay (BCA). 10mg of protein were loaded into the wells of a precast 4-15% SDS-polyacrylamide gels (BioRad) and resolved at 200volts for approximately 1 hour. The cellular proteins were transferred from the polyacrylamide gels by electroblotting onto PVDF membranes for 10 hours at 100mA. PVDF membranes were treated with a solution of 5% non-fat dry milk (NFDM) dissolved in Tris-Buffered Saline containing 0.1% Tween20 (TBST).

Blocked membranes were incubated with the primary antibodies (Basigin 1:500, IDH1m-Dianova 3.33:1000, IDH1 wt 1:500, MGMT 1:500,) overnight at 4°C with shaking. Visualization of specific proteins was accomplished by staining with a goat anti-mouse horseradish peroxidase-labeled antibody (Thermo Scientific) for one hour followed by detection with enhanced chemiluminescence (Pierce Pico Chemiluminescence Reagent). Films were exposed to the blots for thirty seconds and five minutes (Five minute exposure images are figures 6-10). Images were obtained using a Kodak M35A X-OMAT Processor.

The primary antibodies used in this study were as follows: mouse anti-IDH1 (Origene Technologies, Rockville, MD), mouse anti- IDH1-R132H (Millipore, Darmstadt, Germany), mouse anti-MGMT (Thermo Fisher Scientific, United States), mouse anti- Basigin (Genetex), and mouse anti-human IDH1 R132H (Dianova, Germany). The following secondary antibodies were used: donkey anti-mouse Alexaflour 488 (Jackson ImmunoResearch, West Grove, PA) and donkey anti-mouse HRP (Thermo Fisher Scientific, United States).

Histochemistry

Paraffin embedded tumor samples were sectioned at 5μm and transferred to glass slide. Sections were deparaffinazed and rehydrated through graded series of xylene-ethanol. The slides were stained with hematoxylin (Richard-Allen Scientific) and eosin (Richard- Allen Scientific) and then dehydrated through another ethanol-xylene graded series. Following the final xylene wash, the slides were mounted with Cytoseal 60 (Richard-Allan Scientific) and a glass cover slip. Tissue slides were marked, regraded, and imaged by Dr. Weiss at UP Health System- Marquette. All tissue blocks that were

used in this study were confirmed to be GBM tumors.

Immunostaining and confocal imaging

Tissue sections were deparaffinized and rehydrated through graded series of xylene-ethanol and then washed in PBS three times for ten minutes each. Tissue sections were blocked with blocking buffer containing donkey serum (Jackson ImmunoResearch) for one hour. Afterwards, the tissues were incubated with the primary antibodies for Basigin, MGMT, IDH1 R132H, or IDH1 over-night at 4°C (Basigin 1:500, IDH1m-Dianova 1:20, IDH1m- Millipore 1:500, IDH1 wt 1:50, MGMT 1:15). Sections were then incubated with donkey anti-mouse Alexaflour 488 secondary antibody (1:100) (Jackson ImmunoResearch) for one hour in the dark. A second PBS wash was done, three times for ten minutes each, and then ProLong Diamond Antifade Mountant with DAPI (Thermo Scientific) was used to cover slip the sections. Fluorescence intensity of marked malignant spots were visualized with a confocal microscope (Olympus ix81 FV100).

For analysis of the confocal z-stack scans, the software Imaris (Bitplane, Zurich, Switzerland) was used. The software was used to highlight the surface area and intensity of the fluorescence of the nuclei and proteins being tagged. The intensity for each protein was adjusted and expression was determined through the binding of a protein to the nuclei (DAPI stain).

Statistical Analysis

The effects of different protein expression in tumor samples from 5 patients were modeled using "linear mixed models" in R version 3.2.3 (R Core Team 2015)[35]. The package "lme4" was used for the analysis[36]. Two response variables were analyzed

in separate models: “area” (area of the expressed protein, in μm^2; and “intensity”. Intensity is based on the fluorescent signal that is being emitted by the Alexafluor 488 antibody. The fixed effect of primary interest was “protein” (4 levels), but “patient” was also included as random factor to account for variation in protein expression among subjects. The model was of the type where Y= protein + (1 | patient), which models a varying-intercept group effect using the variable “patient”. Least squares means (lsm package in R) and Tukey’s Method were used to estimate means and differences between means adjusted for variation among patients. Linear mixed models were used because the design was unbalanced (some proteins were not present in all patients), and the cells measured were not independent. Linear mixed models are able to model the error structure to avoid violating assumptions inherent in typical ANOVAs.

CHAPTER THREE: RESULTS

Hematoxylin and Eosin Analysis

H&E staining was conducted on the five different GBM tumors that were used in this study. These slides were initially examined and by Dr. Weiss at UPHSM and the boundaries between malignant and nonmalignant tissues were marked. The malignant portions of the tumor were then imaged on the Olympus laser confocal microscope at NMU. Images of these H&E stained slides are shown in Figure 5. Different forms of vascularity and cell formation can be seen throughout the malignant portions of the tissue (Figure 5A-E).

Protein expression within GBM cell lines

Immunoblotting of GBM cell lines with the antibodies used in this study are shown in Figures 6-10. Equivalent amounts of soluble protein for the five cell lines used were loaded in each lane of the immunoblots. The results demonstrate the presence of bands at the anticipated molecular weights for each of the proteins. The DNA repair enzyme MGMT was expressed by the T98 and MSU 1.1 cell lines, but was not detected in any other cell line (Figure 6). The cell surface glycoprotein Basigin was expressed within all lines and clearly demonstrated the presence of two glycosylated forms: a high glycosylated form at ~45-60kDa and a low glycosylated form at ~35 kDa (Figure 7). The IDH1 wild type enzyme was expressed within all cell lines used. The antibody specific for the wildtype IDH1 cannot distinguish between the R132H IDH mutant and

the wild type enzyme. Therefore, the protein sample from the U87MG R132H cell line shows a significant increase in the IDH1 protein as this cell line overexpresses the R132H protein (Figure 8). The IDH1 R132H mutation was expressed within the U87 mutant cell line and was not present in any other (Figure 9). Figure 10 is an immunoblot showing the relative expression for the housekeeping gene GAPDH to show the relative amounts of protein within the cell lysates.

Protein Expression within GBM tissue samples

Figures 11-15 represent images from the immunohistochemistry experiments performed on tissue sections from five different human GBM tumor samples. These different tissue samples are shown in Figure 11 = Block 5625, Figure 12 = Block 3331, Figure 13 = Block 4946, Figure 14 = Block 10168, and Figure 15 = Block 8072). In each series of figures, the tissues were probed with the following antibodies: A = Basigin, B = IDH1 wild type, C = IDH1 R132H (Millipore), D = IDH1 R132H (Dianova), E = MGMT.

All GBM tissues expressed the proteins Basigin, IDH1, IDH1 R132H, and MGMT (Fig11-15). The level of fluorescence within each slide varies in the photos, but can clearly be seen. It should be noted that the IDH1 mutations were imaged using two antibodies from different manufacturers (Dianova and Millipore) and the images using both antibodies are shown. Some of the tissue blocks were initially thought to lack expression of the IDH1 mutation using the Millipore antibody, but when reimaged using the primary antibody from Dianova, staining was observed.

Analysis of Protein Expression in GBM Samples

Figure 16 represents the quantitative data from the fluorescent images shown in figures 11-15. The fluorescent emission from each slide was quantified using the Imaris software package. For this work, the fluorescence from individual cells was measured on Imaris, and the mean values for each protein provided by Imaris were adjusted for the variation among patients. When the data set for protein area was being analyzed, there were variations among the data points. The log of each point was taken and averaged for the final data set. The Tukey Method, a statistical single-step comparison method, was used to compare the means of the proteins in question. These means were also adjusted for the variation among patients. There were significant differences in intensity mean between Basigin and IDH1 m (t ratio= 3.271, df= 493.80, P=0.006), IDH1 m and IDH1 wt (t ratio= -2.679, df= 492.09, P=0.038), and IDH1 m and MGMT (t ratio=-2.830, df= 492.15, P=0.025). No other pairs were significantly different. When the average for log10 of the area means were taken there were significant difference between Basigin and IDH1 wt (P=0.006) and IDH1 wt and MGMT (P=0.0188).

CHAPTER FOUR: DISCUSSION

IDH1 And IDH1 R132H mutant expression in GBM

The use of the human cell lines for immunoblot analysis provided a method for demonstrating the specificity of the antibodies used later in the analysis of the human GBM tissues. For the anti-IDH1 antibodies, what was learned from this analysis was that the anti-IDH1 antibody that is designed to recognize the R132H point mutation was highly specific and did not detect the wild-type IDH1 protein in any of the cell lines used (Figure 9). This antibody detected 10ng of a recombinant IDH1 R132H peptide and the IDH1 R132H isoform overexpressed in the cell line. This cell line was a gift from Horacio Soto at Geffen Cancer Center at UCLA[39]. These cells overexpress this mutant IDH1 R132H isoform (which I will refer to as 'IDH1m') in a background of wild-type IDH1 produced by the cell. Both the wildtype and the mutant isoform possess identical molecular weights and could not be distinguished from each other without the use of monoclonal antibodies. Immunoblotting with the wild-type anti-IDH1 antibody detected the IDH1 protein in all the cell lines, including the IDH1m isomer in the mutant cell line. This is consistent with the fact that this antibody recognizes an epitope that is shared in all forms of the IDH1 protein (mutant and wild-type). Thus, in lane 2 of figure 8, the antibody produced a strong signal as it recognized epitopes on the over-expressed recombinant protein. Within human tissues, the presence of the R132H mutation leads to the production of the oncometabolite 2-hydroxyglutarate (2-HG) and often results in the loss of the wild-type IDH1 allele [10]. The presence of fluorescent signals on the same GBM tissues using both wildtype and

mutant IDH1 antibodies suggests that both isoforms are present within the tissues (Figures 11-16, panels B, C & D). However, it is also possible that some of the protein recognized by the wild-type antibody actually represents the IDH1m isoform. Unfortunately, clarification of this issue was outside of the technical ability in this study. Nonetheless, the immunoreactivity with the IDH1m antibody is highly specific, and the results from Figure 11-16 panel D clearly show the presence of this mutant isoform. The significance of this result is that this isoform is usually found in low-grade brain tumors and secondary GBMs, and patients with this mutation experience a longer survival rate with full resection of the tumor and aggressive chemotherapy.

Basigin expression in GBMs

The cell surface glycoprotein named Basigin has recently been an area of interest as a cancer antigen[34]. Known also as extracellular matrix metalloproteinase inducer (EMMPRIN) or CD147, the expression of basigin protein in GBM tumors is generally very high[34]. Elevated Basigin levels correlate with increased angiogenesis, cell proliferation and cell invasion leading to more aggressive tumors with a more fatal diagnosis[37]. Immunostaining of the GBM tissues demonstrated a significant difference in the expression levels of Basigin and IDH1m, with IDH1m expression reduced in cells with elevated Basigin. This data supports our hypothesis that these two proteins are inversely correlated and may have separate and opposing effects in tumor growth. Further research is needed to show the exact correlation between the two proteins. If there is a decreased amount of Basigin being expressed when IDH1m is present, either in a heterozygous or homozygous fashion, this would help explain the reason why GBMs with this mutation respond to treatment. The decreased amount of Basigin

would not promote as much angiogenesis and cell proliferation, therefore forming a less aggressive and slower growing tumor.

MGMT Expression

Immunoblot analysis of the DNA repair enzyme MGMT within the human cell lines demonstrated that this protein is expressed in the GBM cell line T98 and the human fibroblast cell line MSU 1.1. A lack of MGMT expression in particular cells is commonly a result of MGMT promoter methylation status, as the promoter methylation silences MGMT gene expression [40]. The cell lines LN229 and U87MG did not express MGMT protein suggesting that the MGMT promoters in these cell lines are methylated. To confirm this result, additional experiments would be necessary, including bisulfite DNA sequencing to demonstrate the methylation of cytosine residues within the MGMT promoter. Cells that maintain expression of the MGMT gene can repair DNA damaged by alkylating agents such as TMZ. Therefore, blocking MGMT production or function would enhance the effectiveness of chemotherapeutics like TMZ. Based upon the statistical analysis of the MGMT expression in GBM tissues (Tukey's test), MGMT levels are significantly reduced in cells expressing of IDH1m. Once again, this pattern of protein expression supports the stated hypothesis that MGMT levels are inversely correlated with IDH1m expression levels. At this time, we cannot yet explain how the presence of IDH1 R132H enzyme affects expression levels of Basigin or MGMT, nor how it may alter tumor growth and repair.

Protein Expression within Human GBM tumors

There was variation within the protein expression in the GBM tissues samples. When observing the differences in mean intensity of each protein, there was a

significant difference between IDH1m and all other proteins. Basigin, IDH1wt, and MGMT were not significantly different from one another. Among the five patients, there was overall stronger fluorescent signal for Basigin, IDH1wt and MGMT. When examining the area of each protein in the tissues, there were significant differences between IDH1 wt and MGMT, and IDH1 wt and Basigin. Since this study was mainly comparing the difference of expression in IDH1 mutation and Basigin expression, it was surprising to find differences between IDH1 wt and other proteins. The difference between the mean intensity and area could be explained by the difference in measurement. Mean intensity is measuring the brightness of the secondary antibody and the area is measuring the size of the protein bound by the antibodies. This may not give the most accurate depiction of what is truly happening within the tumors.

In future studies it would be best to utilize different primary antibodies that originate from different host animals. This would allow us to probe each tissue block with multiple antibodies simultaneously to allow for the measurement of protein expression in each cell of a tumor. This approach would allow for a more powerful statistical analysis of the correlation between protein expression, tumor growth and patient survival.

CONCLUSION

In conclusion, this study has shown that there is a difference among IDH1 mutation expression and Basigin, IDH1 wt and MGMT. Further investigation on these findings is needed and a larger patient group should be used. Patient history may also be useful in future studies to assist in background knowledge of the patients. Having the background knowledge of patients may allow for more of a selective process when

choosing tumor blocks and allow for a control group (GBM with IDH1m and without). Finding more correlations between these proteins may lead to better treatments and more advantageous diagnoses leading to a longer overall survival, and possibly, better quality of life for GBM patients. This could be accomplished by increasing the amount of tumor suppressor gene mutations and oncogene overexpression that are tested for after tumor resection. Also, adding to the forms of treatment and possible chemotherapies that target other aspects of GBM tumors.

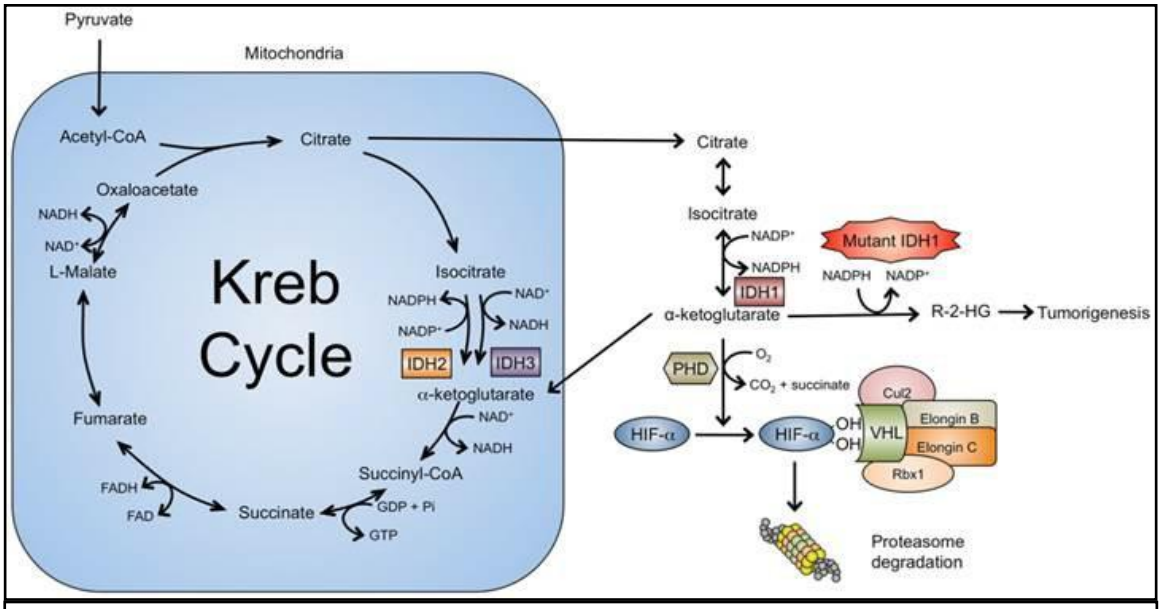

Figure 1. Isocitrate dehydrogenase (IDH) enzyme function in human cells. This figure illustrates the role of the IDH enzymes in cellular metabolism in both the mitochondria and the cytoplasm of the cell. The enzyme IDH1 primarily functions in the cytoplasm of the cell where it is involved in the production of NADPH and α-ketoglutarate. Image adapted from Dimitrov et al. *Int J Med Sci* 2015; 12(3):201-213. doi:10.7150/ijms.11047

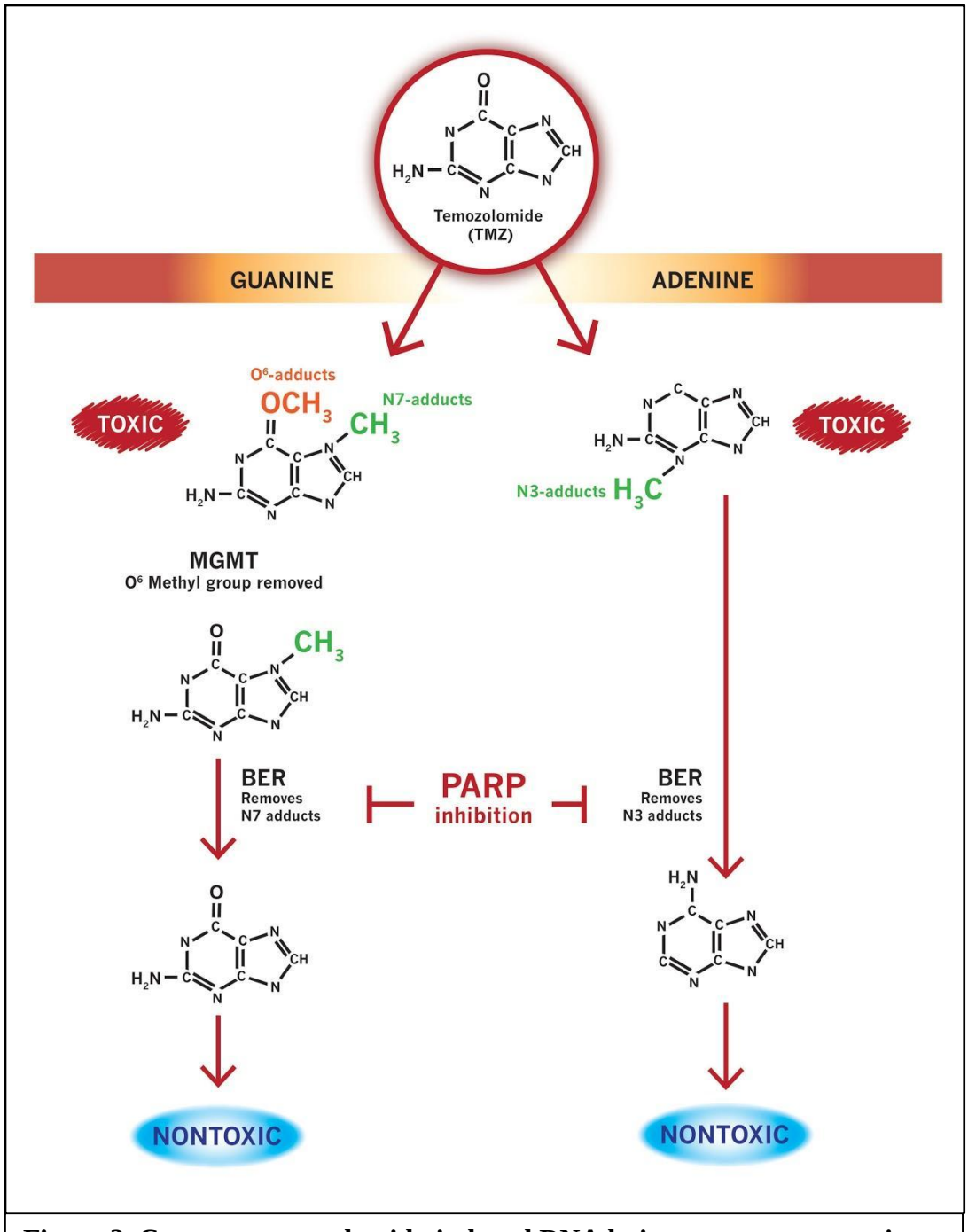

Figure 2. Common temozolomide-induced DNA lesions appear on guanine and adenine. N7-methylguanine, N3-methyladenine and O6-methylguanine DNA adducts account for roughly 70%, 10% and 5% of these lesions respectively. The enzyme MGMT mediates removal of the O6-methylguanine adducts. Adapted from Lawrence et al 2015 [4].

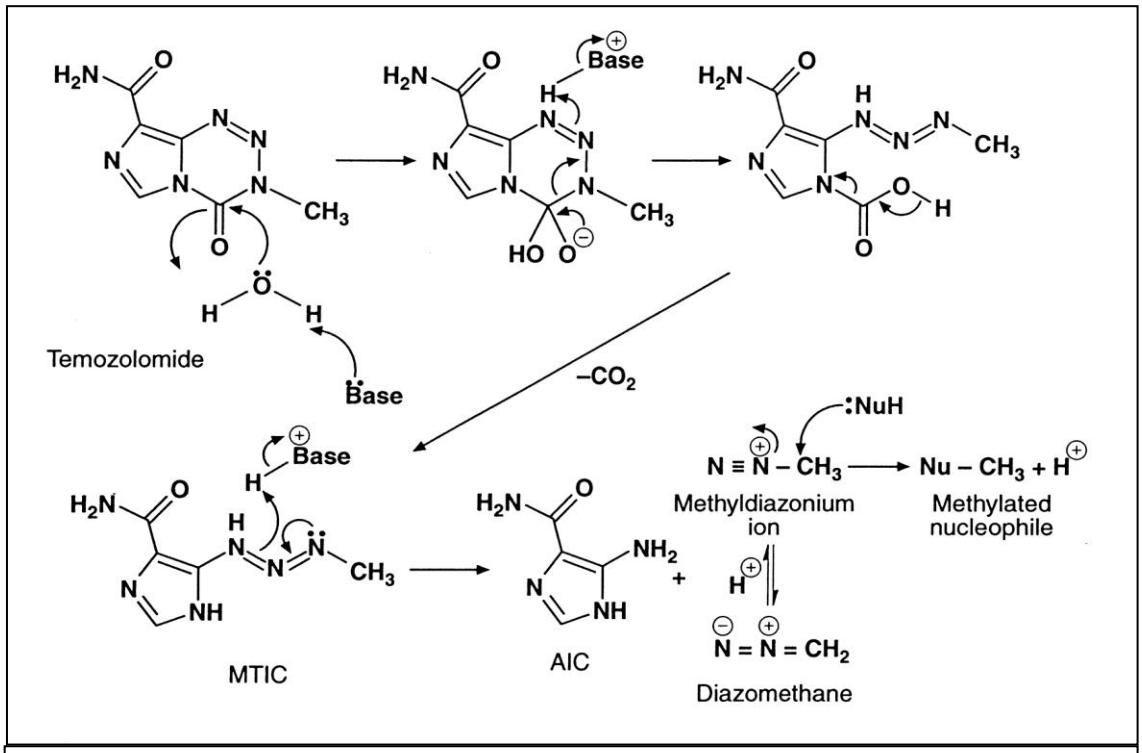

Figure 3. Temozolomide is converted to MTIC within the body and contributes methyl or alkyl chemical groups on DNA. Adapted from Agarwala et al. *The Oncologist* April 2000 vol. 5 no. 2 144-151.

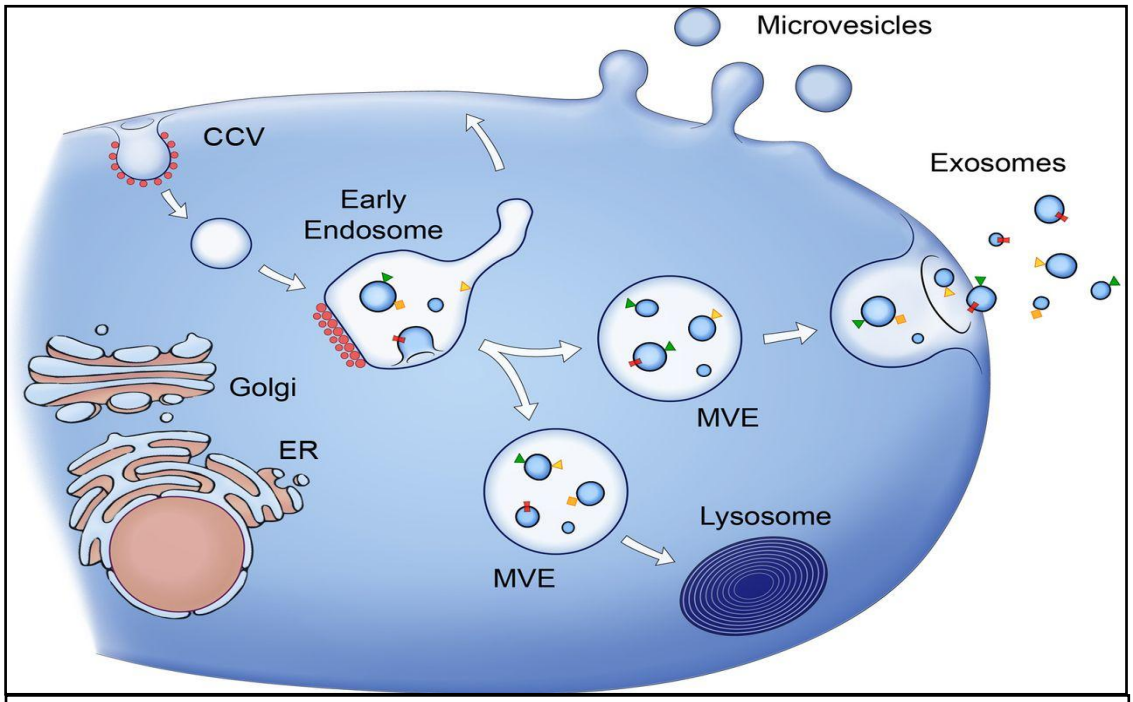

Figure 4. Microvesicles and exosomes are membrane vesicles released from cells to the extracellular space. Image adapted from Raposo & Stoorvogel *J. Cell Biol. Vol. 200 No. 4 373–383 www.jcb.org/cgi/doi/10.1083/jcb.201211138*

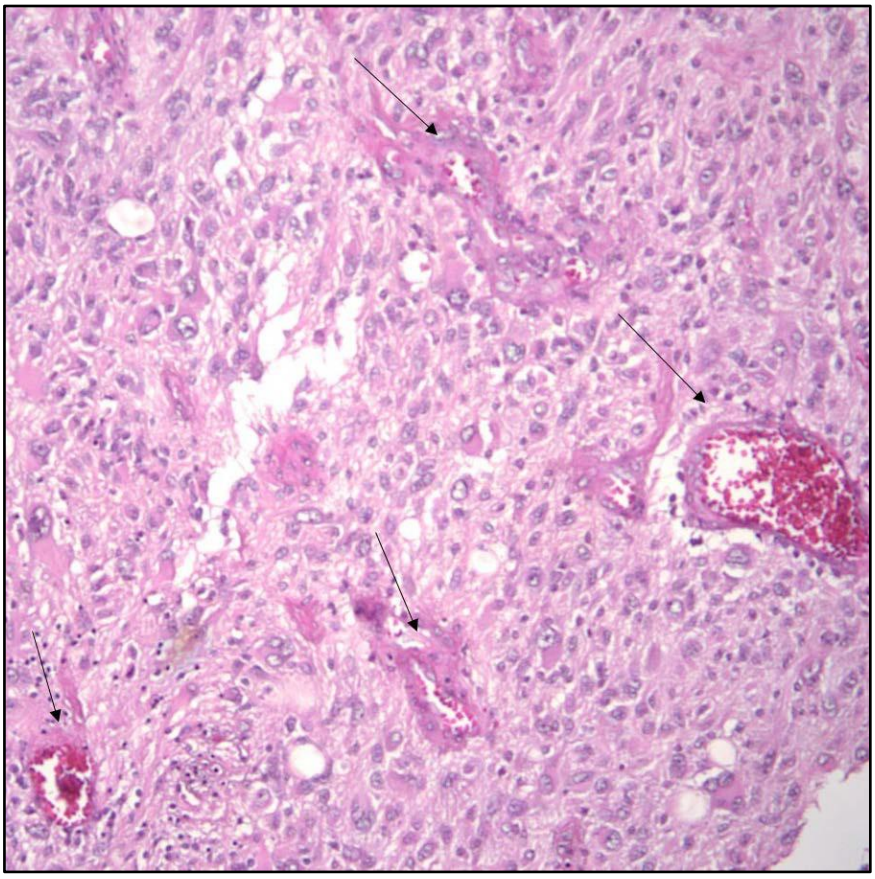

Figure 5A. H&E Staining from Block 5652. This image illustrates increased blood vessel growth (arrows) and formation and increased cell density within the sample. High vascularity is a common sign of GBM tumors and many tumors will develop their own blood supply when they become large enough.

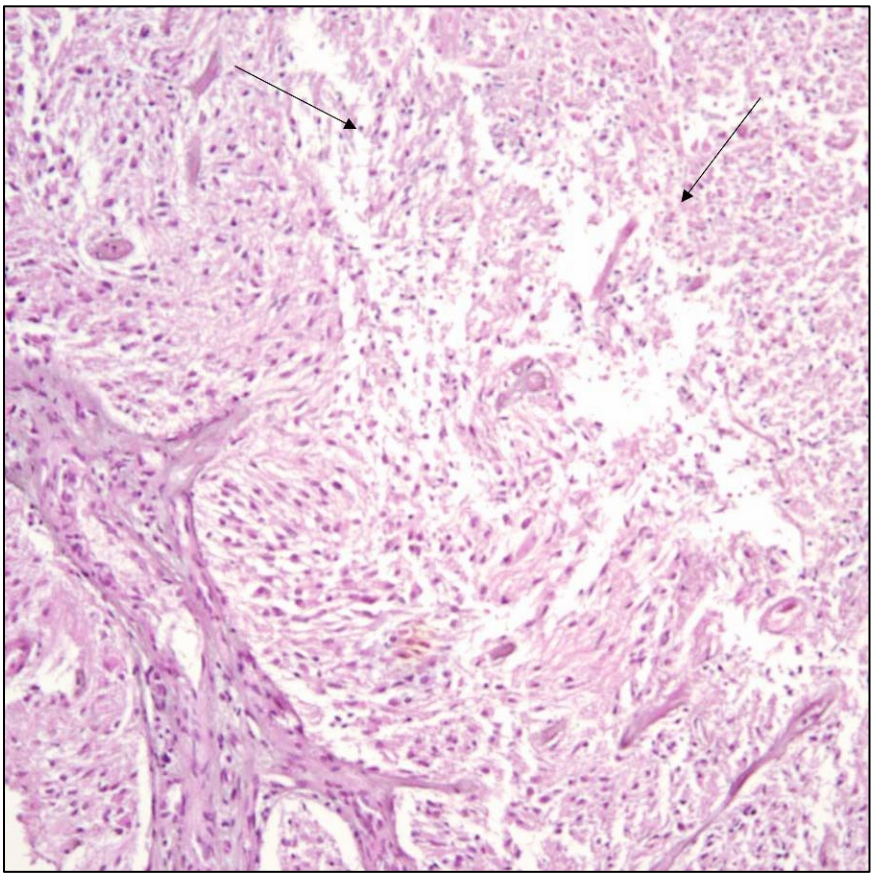

Figure 5B. H&E Staining from Block 3331. This image shows high cell density on the left side of the image and necrosis (arrows) on the right where the arrows are located. Necrosis is a very common characteristic of GBM tumors.

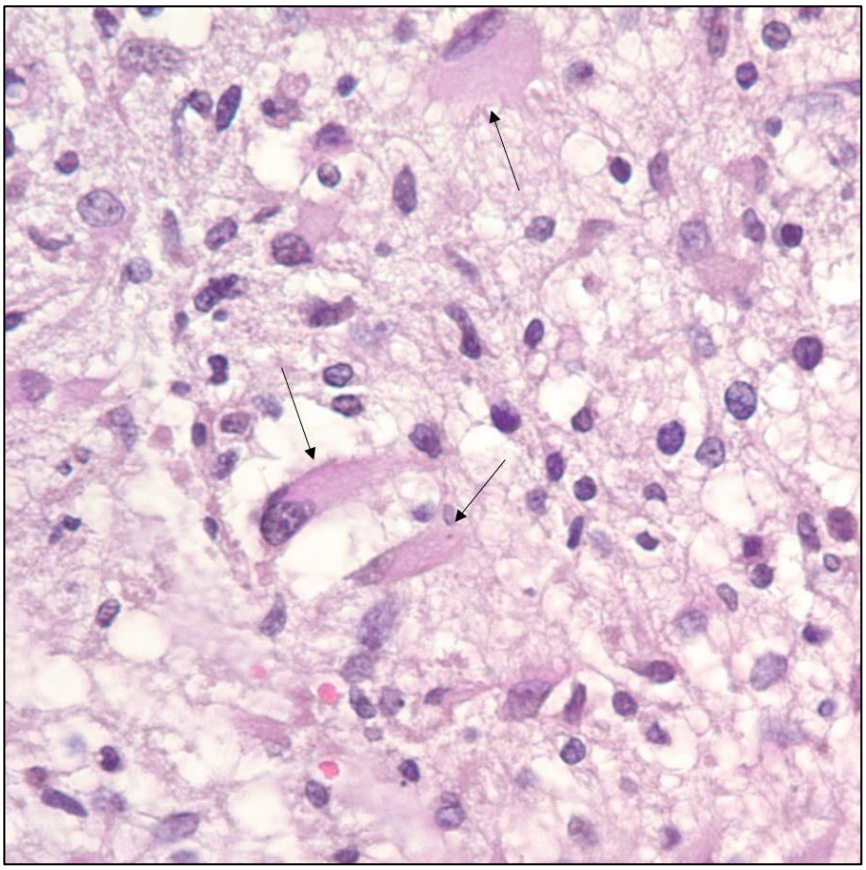

Figure 5C. H&E Staining from Block 4946. This image of a GBM tumor shows gemistocytic astrocytes (arrows) that are characterized by their swollen cytoplasmic mass. These types of astrocytes are present when there is scarring within the CNS tissue and can lead to confusion, drowsiness, stupor or coma.

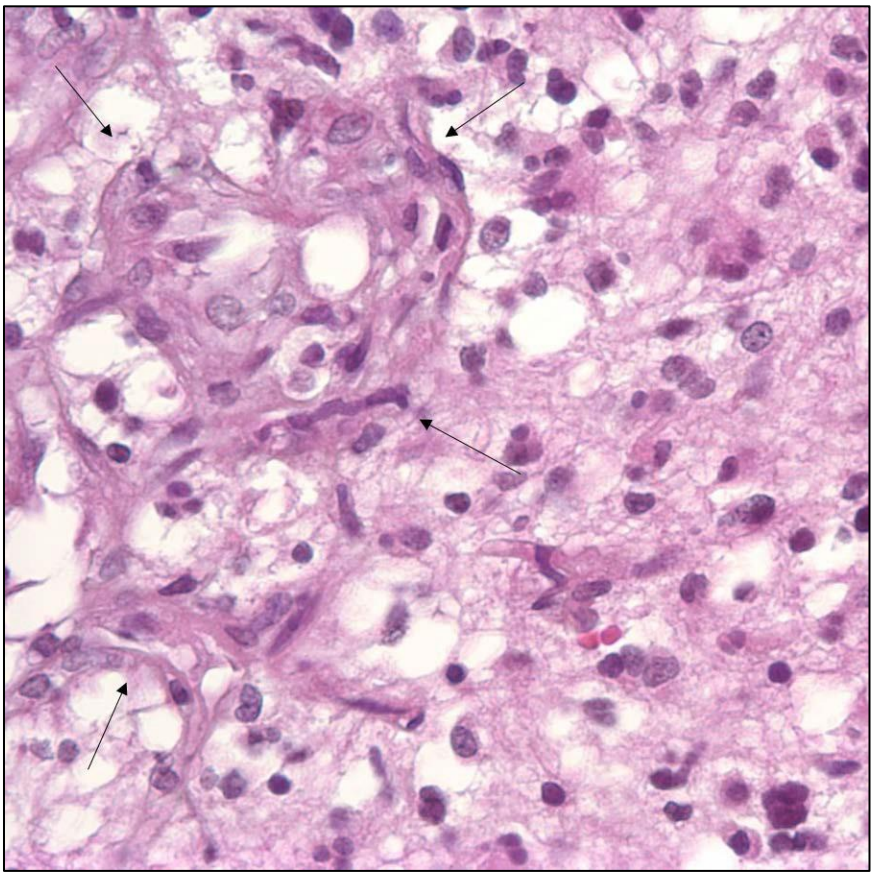

Figure 5D. H&E Staining from Block 10168. This tissue is displaying glomeruloid vascularity, indicated by the arrows. This form of vasculature is conducive with angiogenesis and can signify the presence of elevated levels of vascular endothelial growth factor (VEGF) within a tumor.

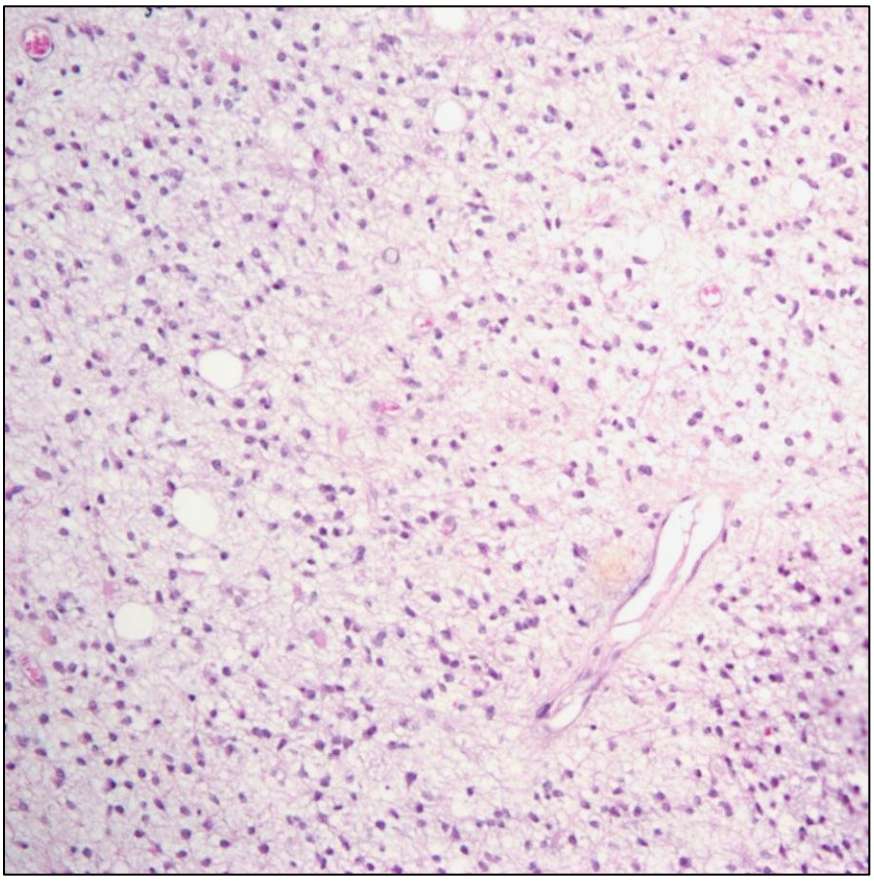

Figure 5E. H&E Staining from Block 8072. This GBM tissue is displaying high cell density and this is believed to be the outer area of the tumor.

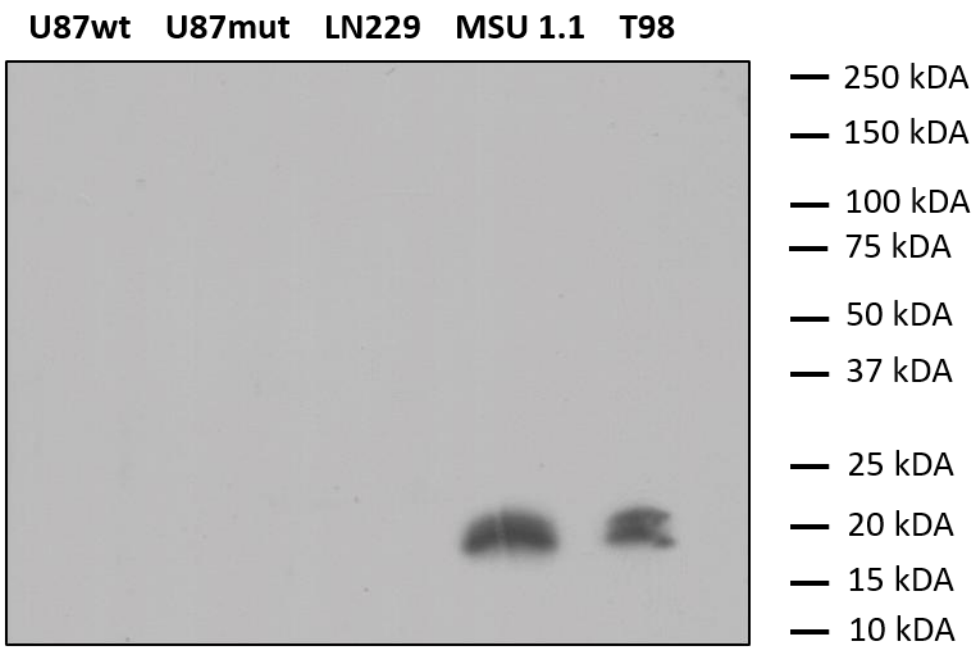

Figure 6. Immunoblotting of human cell lines with the MGMT antibody. This antibody recognizes the DNA repair enzyme O-6-methylguanine-DNA methyltransferase (MGMT) protein. The absence of this DNA repair enzyme in some of the GBM cell lines (eg. U87 and LN229) is a common occurrence in brain tumors Molecular weight standard sizes are shown on the right. The anticipated size of the MGMT protein is 21kDa.

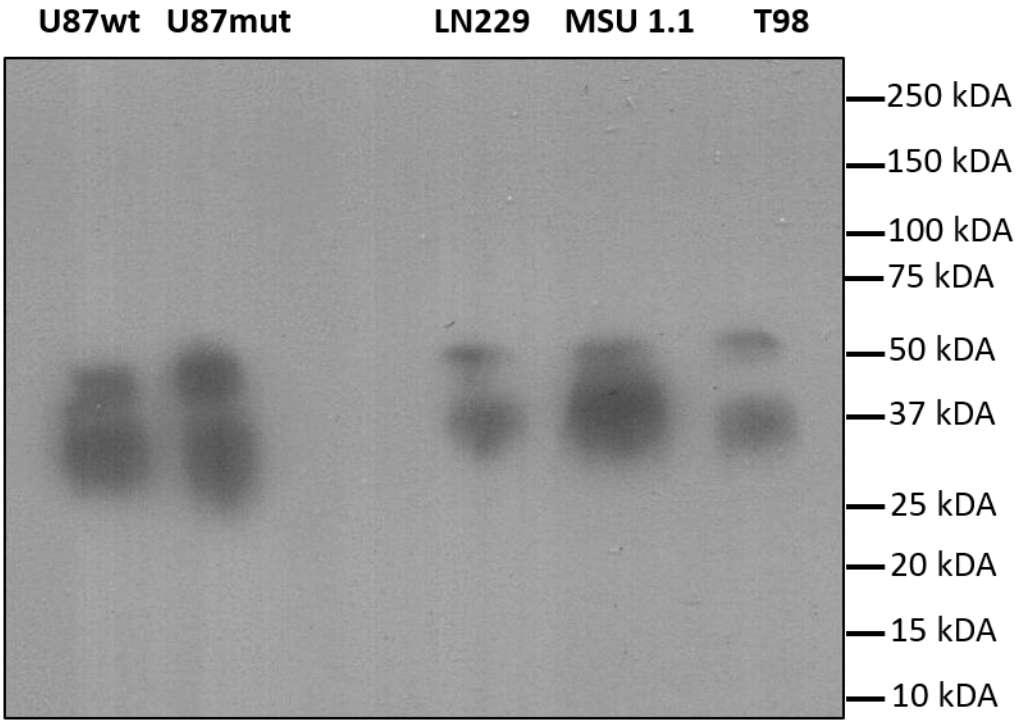

Figure 7. Immunoblotting of human cell lines with the Basigin antibody. This antibody recognizes the all differentially glycosylated isoforms of human Basigin protein. Molecular weight standard sizes are shown on the right. The anticipated size of glycosylated Basigin ranges from 30-60kDa.

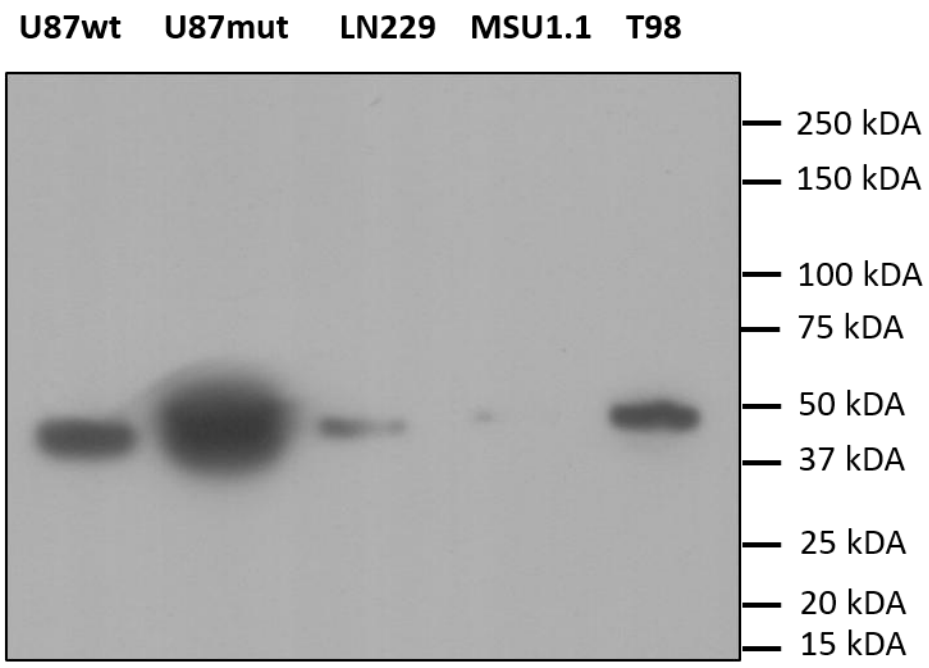

Figure 8. Immunoblotting of human cell lines with the IDH1 antibody. This antibody recognizes the enzyme Isocitrate Dehydrogenase-1 (IDH1). Molecular weight standard sizes are shown on the right. The anticipated size of IDH1 protein is 46kDa.

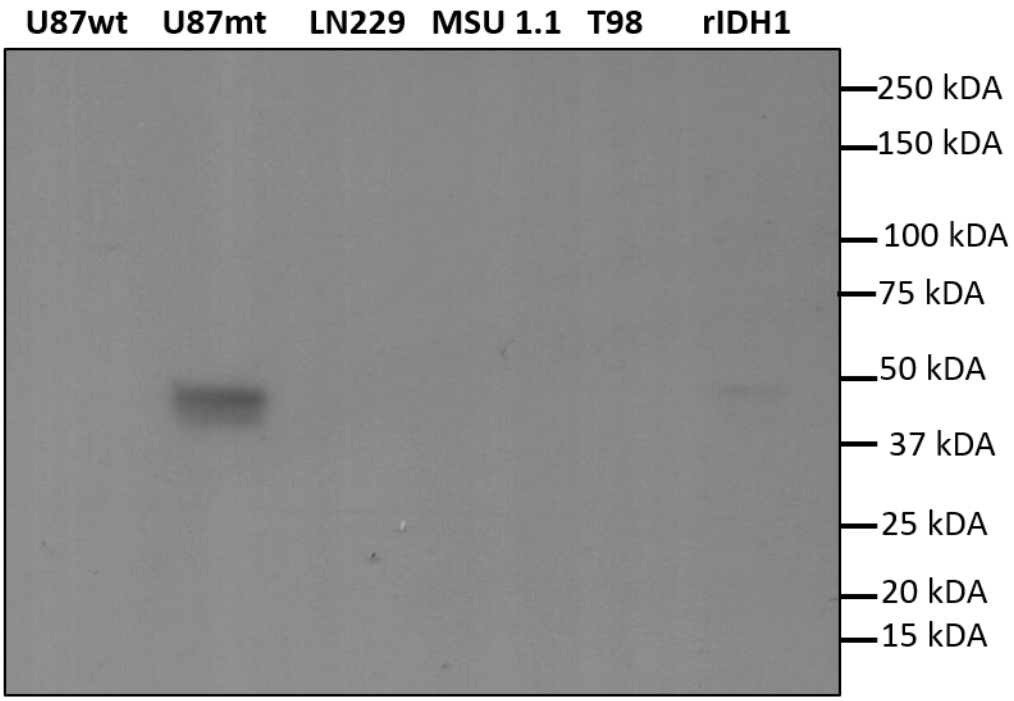

Figure 9. Immunoblotting of human cell lines with the IDH1 mutant antibody. This antibody recognizes only the IDH1 isoform containing an Arginine-to-Histidine mutation at amino acid 132 of Isocitrate Dehydrogenase-1 (IDH1 R132H). 10ng of a recombinant IDH1 R132H peptide was used in the lane on the right as a positive control for immunoblotting. Molecular weight standard sizes are shown on the right. The anticipated size of IDH1 protein is 46kDa.

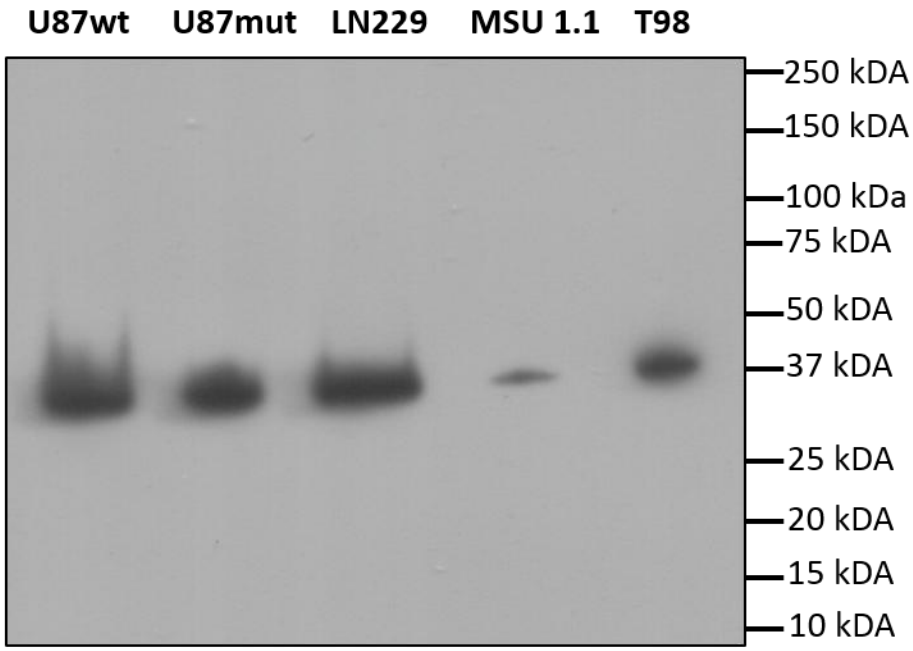

Figure 10. Immunoblotting of human cell lines with the GAPDH antibody. The relative expression of the housekeeping gene glyceraldehyde-3-phosphate dehydrogenase (GAPDH) was tested to demonstrate relative levels of protein present within the cell lysates. Molecular weight standard sizes are shown on the right. The anticipated size of GAPDH is 37kDa.

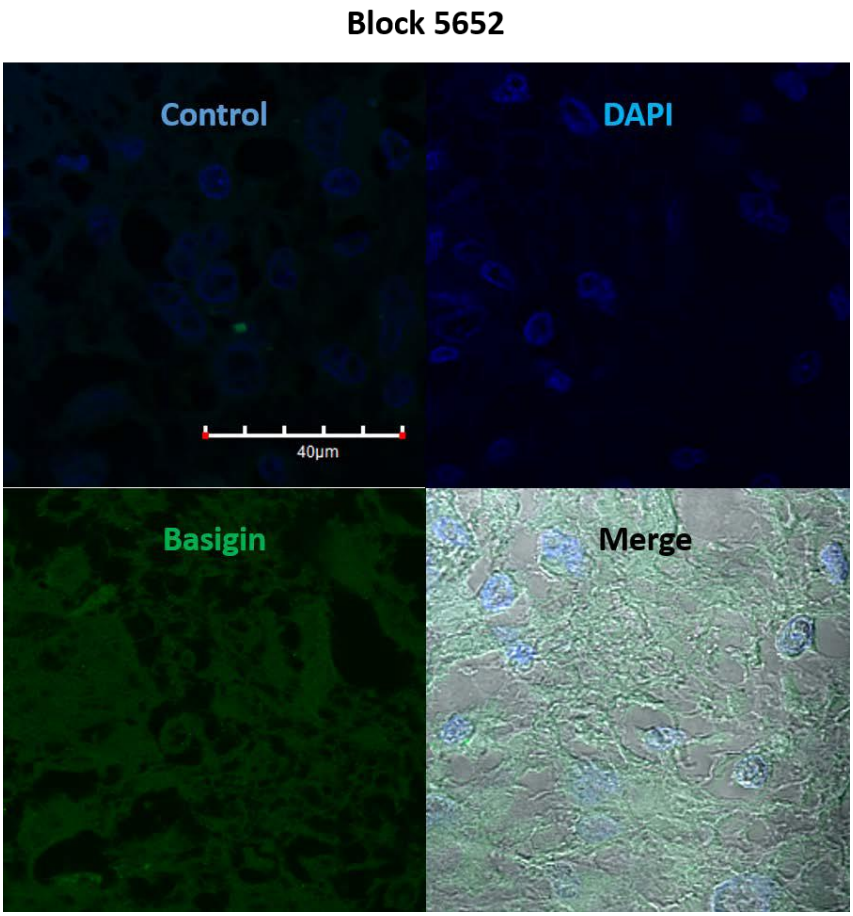

Figure 11A. Immunofluorescence of basigin in block 5625. The control image is showing the absence of the secondary fluorescent antibody binding. The merged image is showing both DAPI staining and basigin expression, along with the outlines of the cell bodies.

Block 5625

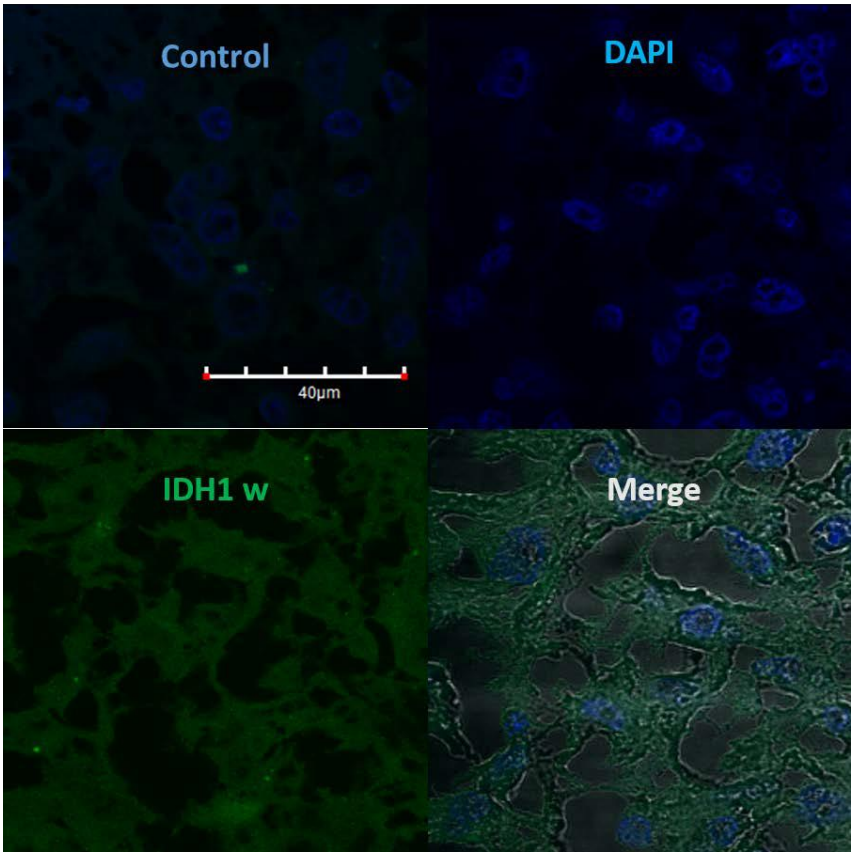

Figure 11B. Immunofluorescence of IDH1 wild type in block 5625. The control image is showing the absence of the secondary fluorescent antibody binding. The merged image is showing both DAPI staining and IDH1 wild type expression, along with the outlines of the cell bodies.

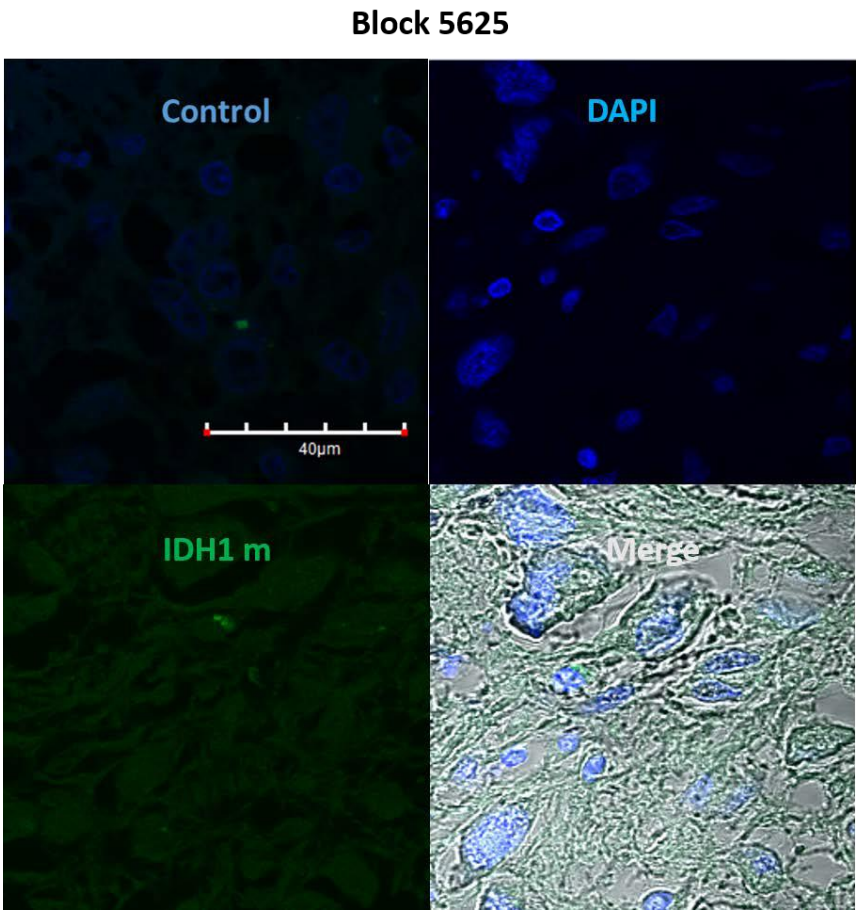

Figure 11C. **Immunofluorescence of IDH1 mutation in block 5625.** The control image is showing the absence of the secondary fluorescent antibody binding. The merged image is showing both DAPI staining and IDH1 mutation expression, along with the outlines of the cell bodies.

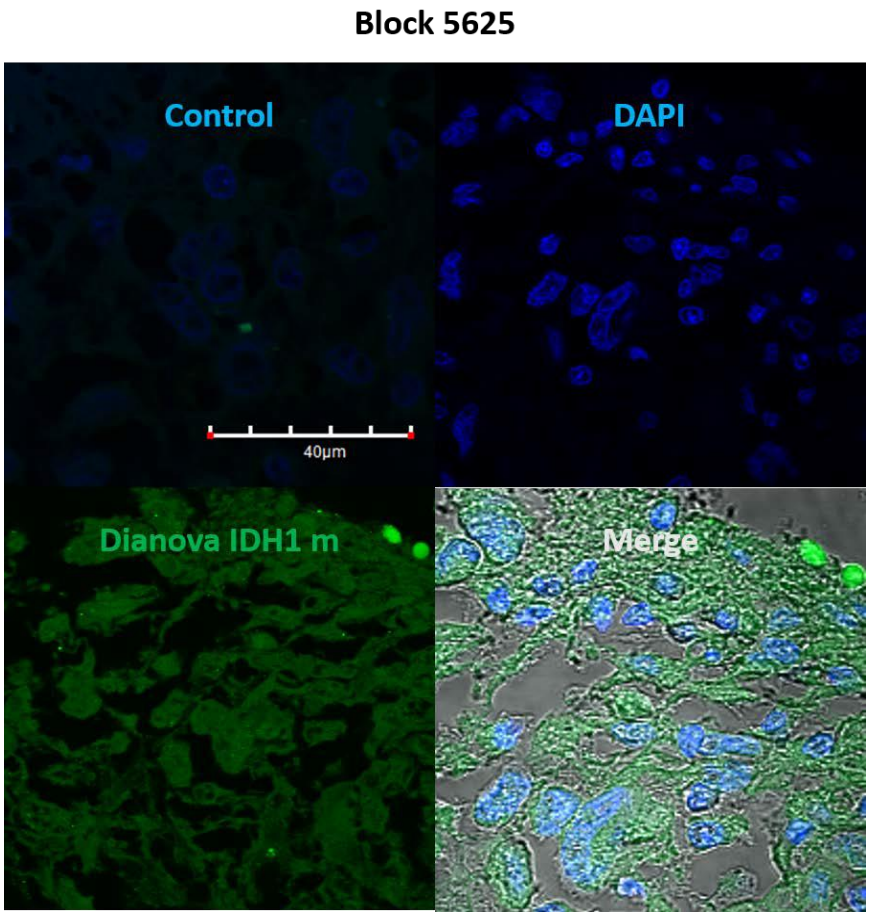

Figure 11D. **Immunofluorescence of IDH1 mutation in block 5625**. The control image is showing the absence of the Dianova fluorescent antibody binding. The merged image is showing both DAPI staining and IDH1 mutation expression, along with the outlines of the cell bodies.

Block 5625

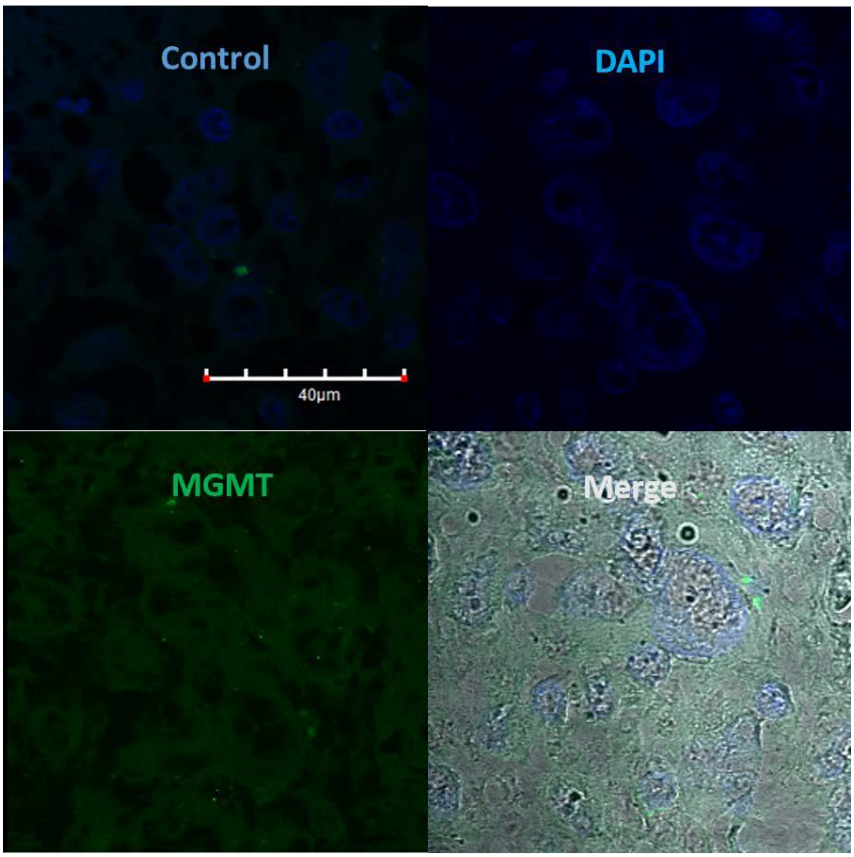

Figure 11E. **Immunofluorescence of MGMT in block 5625**. The control image is showing the absence of the secondary fluorescent antibody binding. The merged image is showing both DAPI staining and MGMT expression, along with the outlines of the cell bodies.

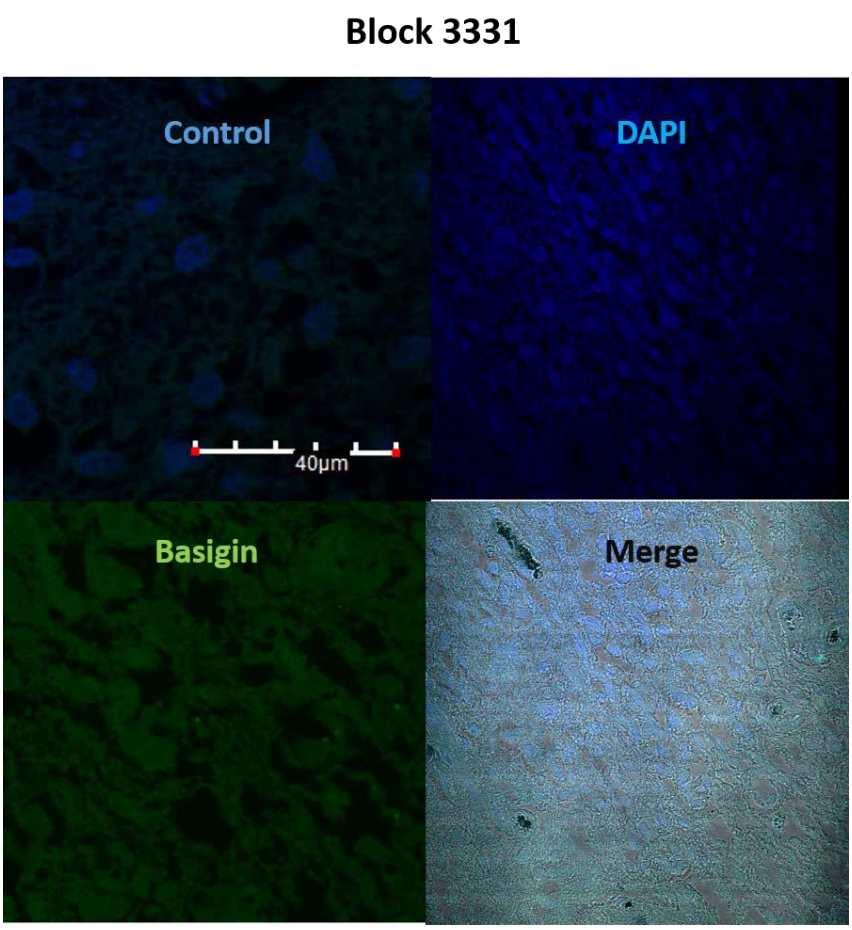

Figure 12A. **Immunofluorescence of Basigin in block 3331**. The control image is showing the absence of the secondary fluorescent antibody binding. The merged image is showing both DAPI staining and Basigin expression, along with the outlines of the cell bodies.

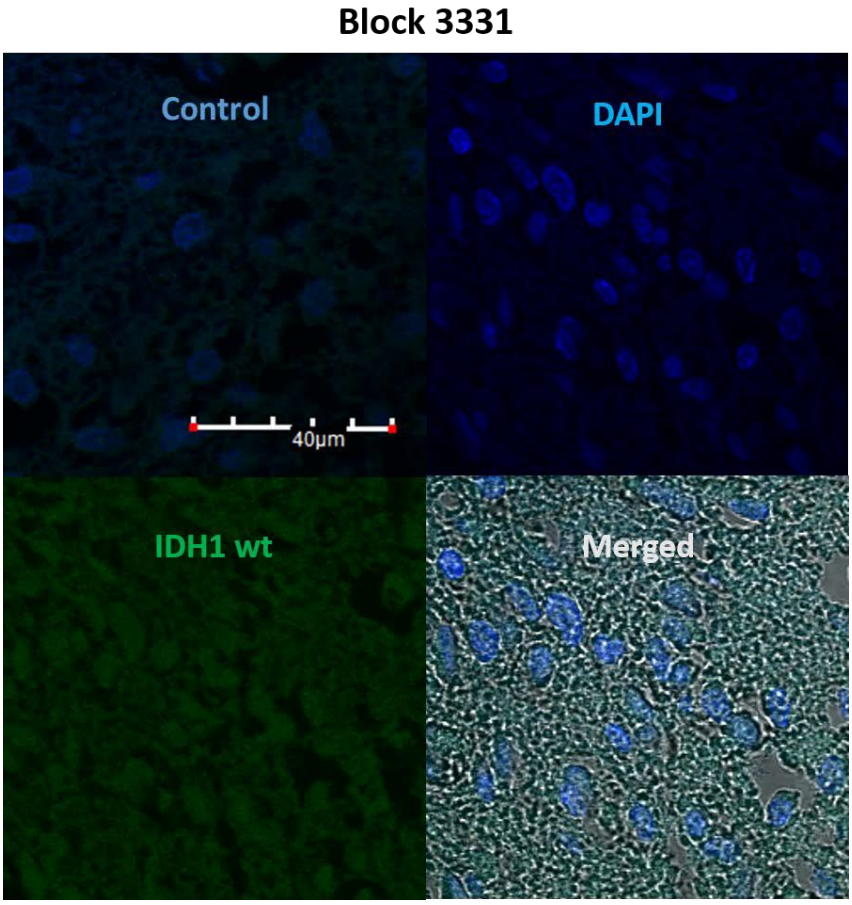

Figure 12B. **Immunofluorescence of IDH1 wild type in block 3331**. The control image is showing the absence of the secondary fluorescent antibody binding. The merged image is showing both DAPI staining and IDH1 wild type expression, along with the outlines of the cell bodies.

Block 3331

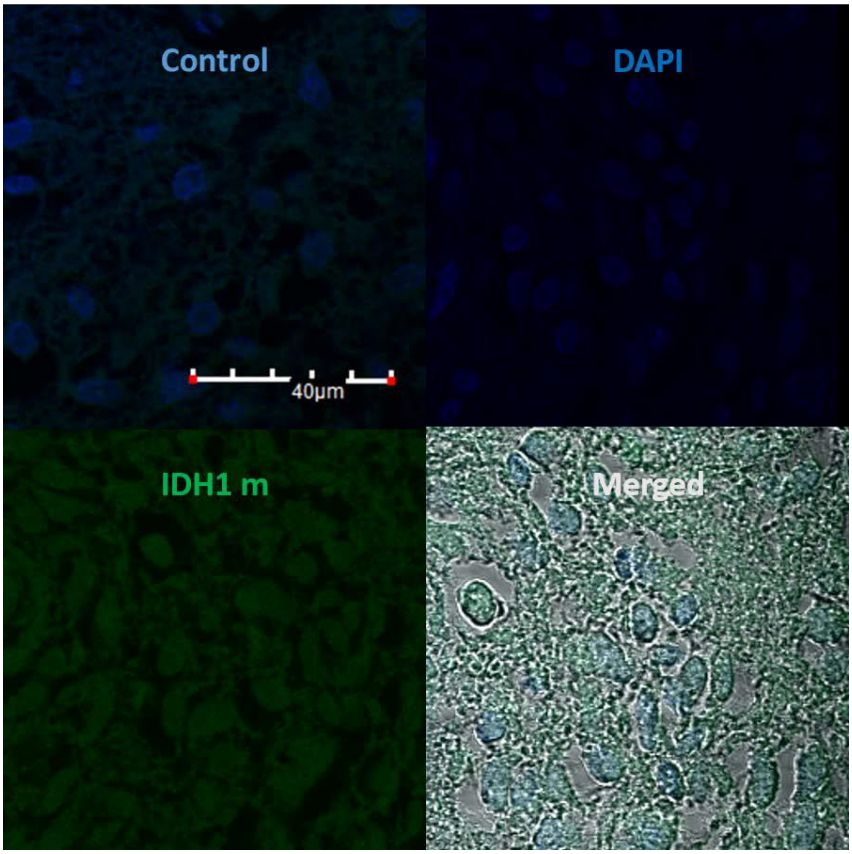

Figure 12C. Immunofluorescence of IDH1 mutation in block 3331. The control image is showing the absence of the secondary fluorescent antibody binding. The merged image is showing both DAPI staining and IDH1 mutation expression, along with the outlines of the cell bodies.

Block 3331

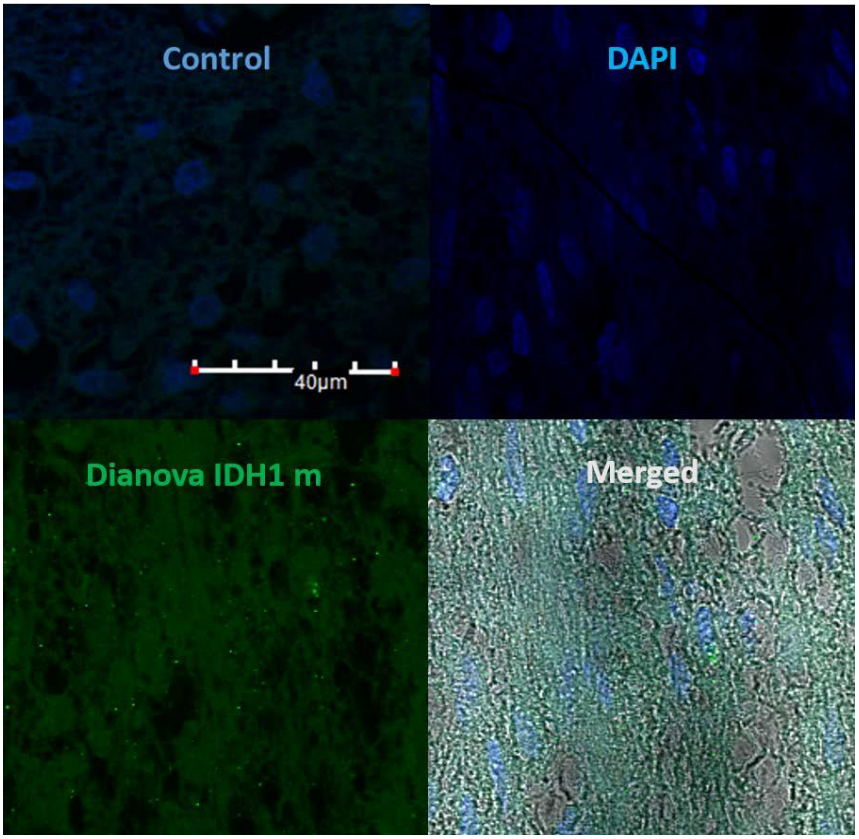

Figure 12D. Immunofluorescence of IDH1 mutation in block 3331. The control image is showing the absence of the Dianova fluorescent antibody binding. The merged image is showing both DAPI staining and IDH1 mutation expression, along with the outlines of the cell bodies.

Block 3331

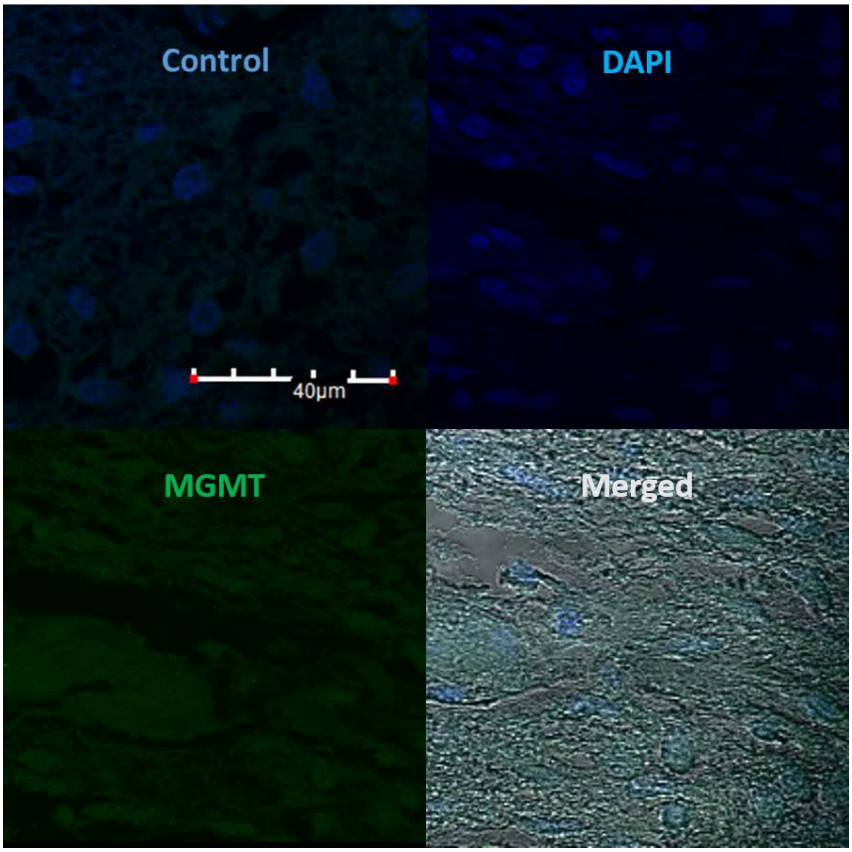

Figure 12E. **Immunofluorescence of MGMT in block 3331.** The control image is showing the absence of the secondary fluorescent antibody binding. The merged image is showing both DAPI staining and MGMT expression, along with the outlines of the cell bodies.

Block 4946

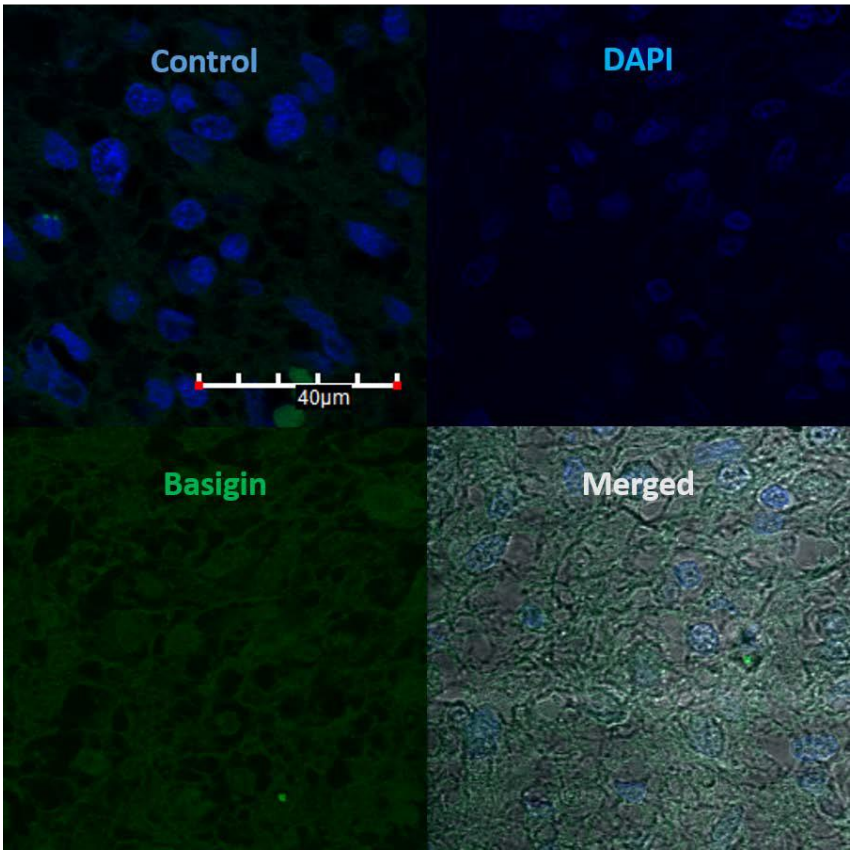

Figure 13A. Immunofluorescence of basigin in block 4946. The control image is showing the absence of the secondary fluorescent antibody binding. The merged image is showing both DAPI staining and basigin expression, along with the outlines of the cell bodies.

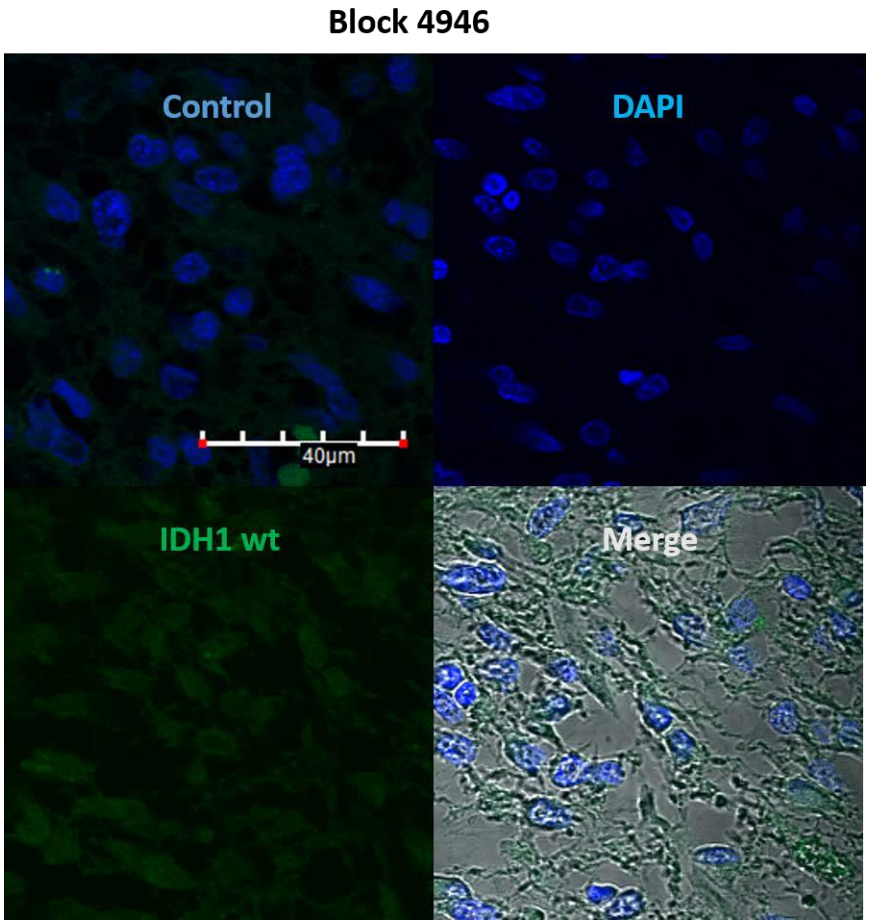

Figure 13B. **Immunofluorescence of IDH1 wild type in block 4946**. The control image is showing the absence of the secondary fluorescent antibody binding. The merged image is showing both DAPI staining and IDH1 wild type expression, along with the outlines of the cell bodies.

Block 4946

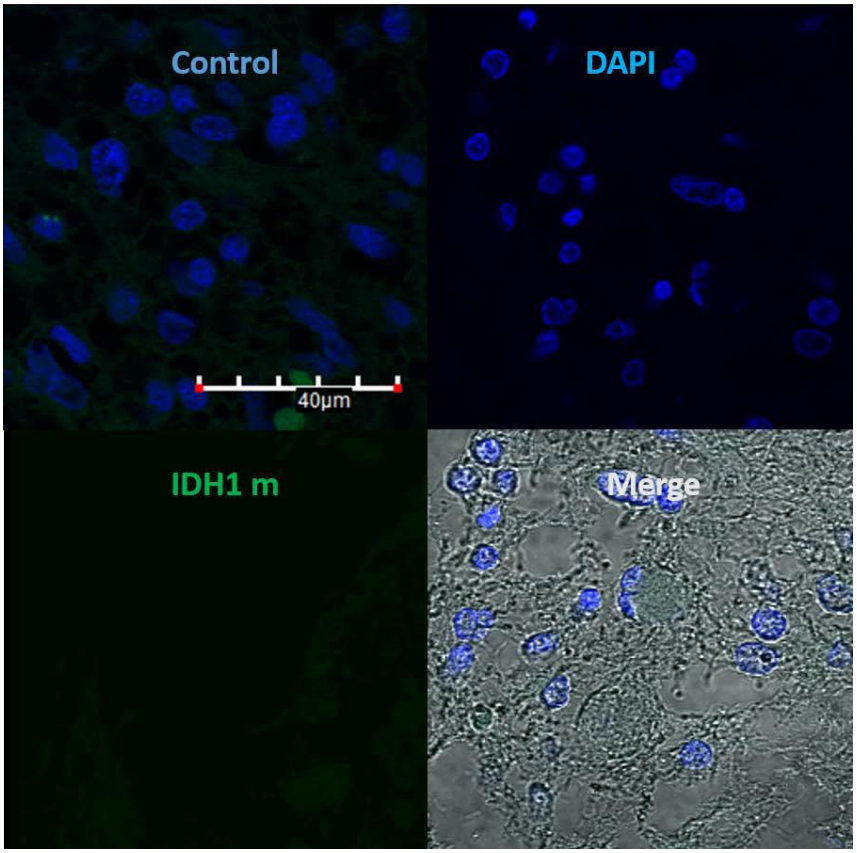

Figure 13C. **Immunofluorescence of IDH1 mutation in block 4946.** The control image is showing the absence of the secondary fluorescent antibody binding. The merged image is showing both DAPI staining and IDH1 mutation expression, along with the outlines of the cell bodies.

Block 4946

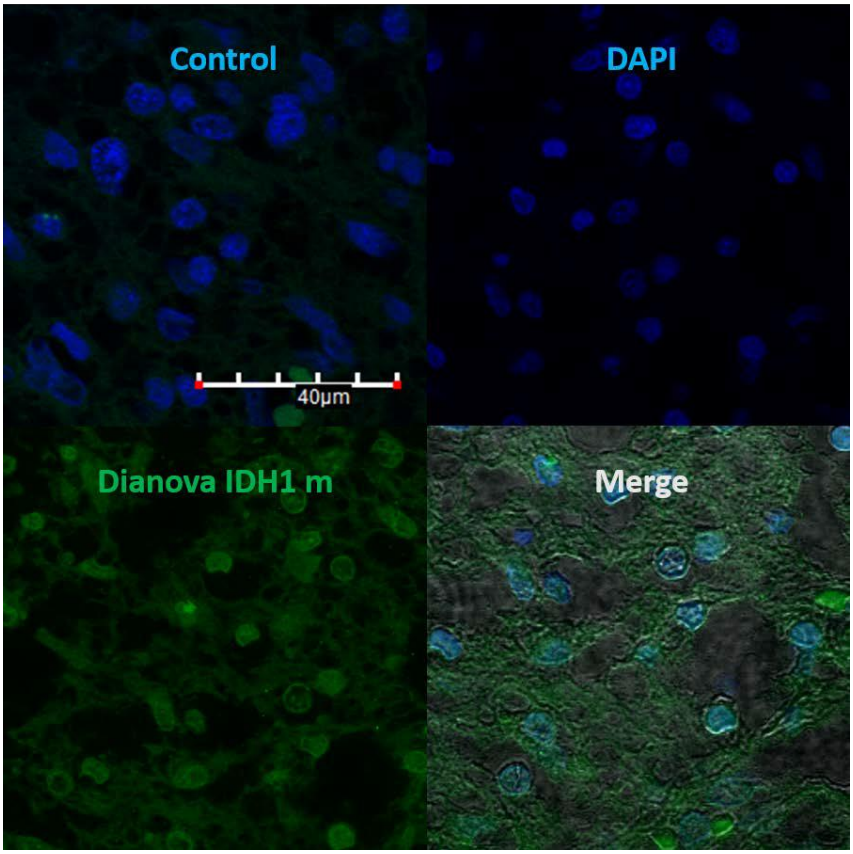

Figure 13D. **Immunofluorescence of IDH1 mutation in block 4946**. The control image is showing the absence of the Dianova fluorescent antibody binding. The merged image is showing both DAPI staining and IDH1 mutation expression, along with the outlines of the cell bodies.

Block 4946

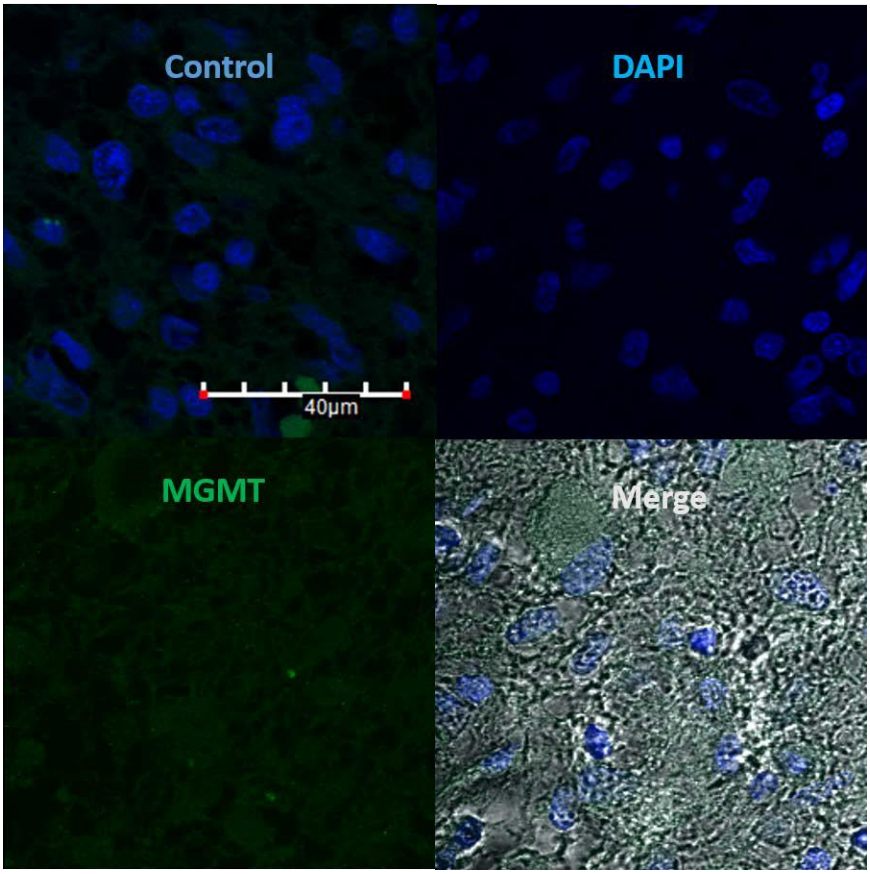

Figure 13E. **Immunofluorescence of MGMT in block 4946.** The control image is showing the absence of the secondary fluorescent antibody binding. The merged image is showing both DAPI staining and MGMT expression, along with the outlines of the cell bodies.

Block 10168

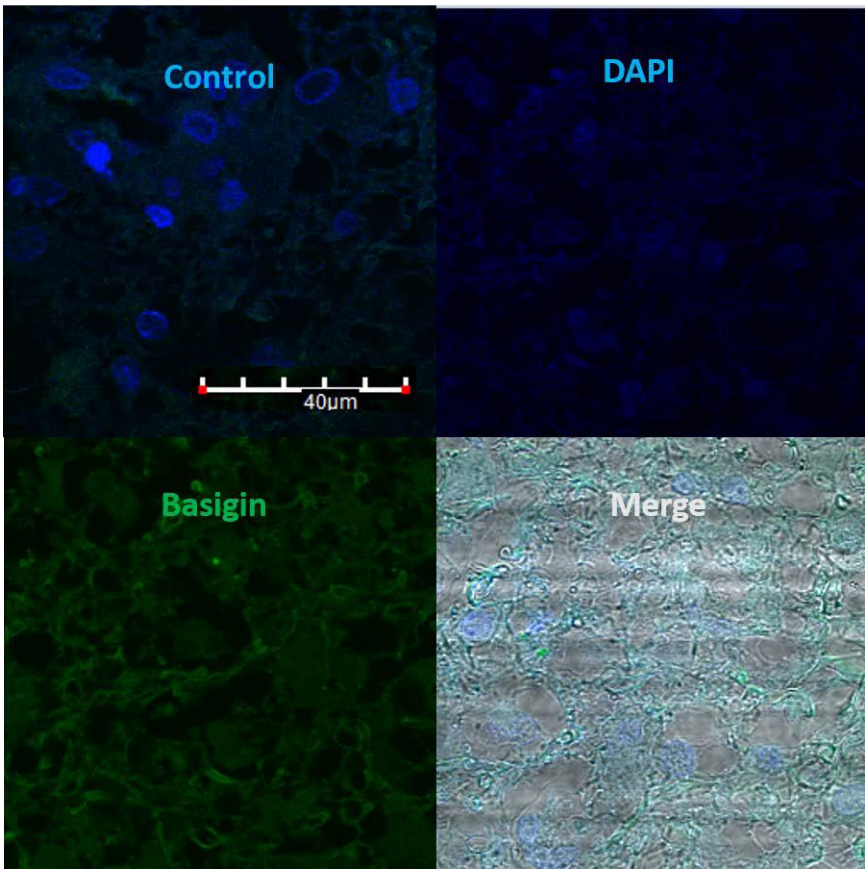

Figure 14A. **Immunofluorescence of Basigin in block 10168**. The control image is showing the absence of the secondary fluorescent antibody binding. The merged image is showing both DAPI staining and Basigin expression, along with the outlines of the cell bodies.

Block 10168

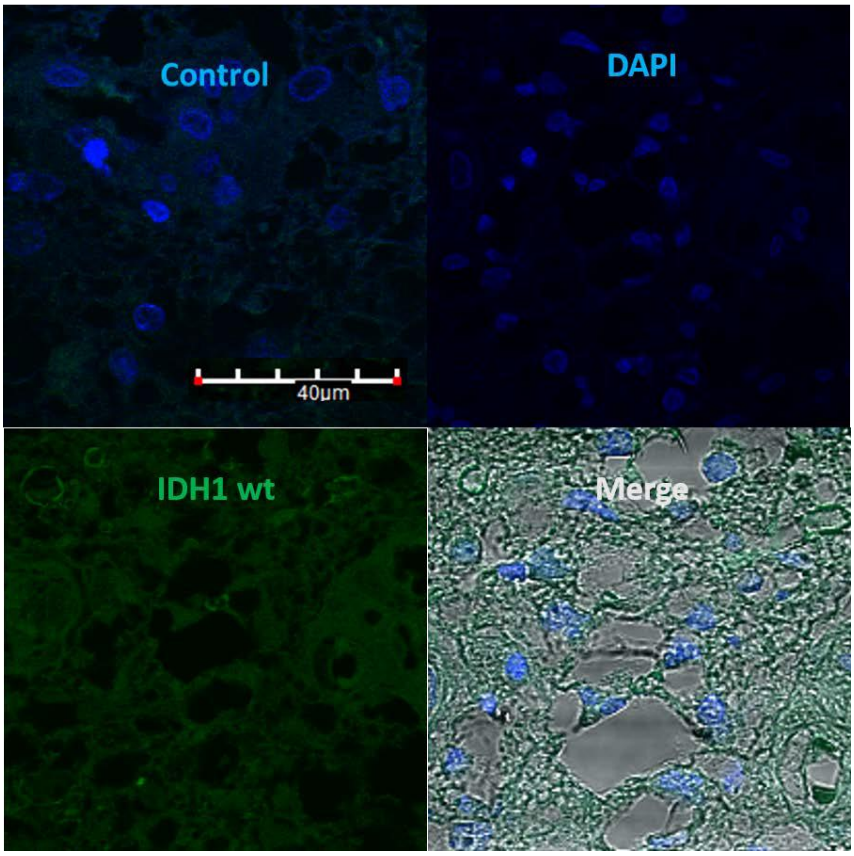

Figure 14B. **Immunofluorescence of IDH1 wild type in block 10168**. The control image is showing the absence of the secondary fluorescent antibody binding. The merged image is showing both DAPI staining and IDH1 wild type expression, along with the outlines of the cell bodies.

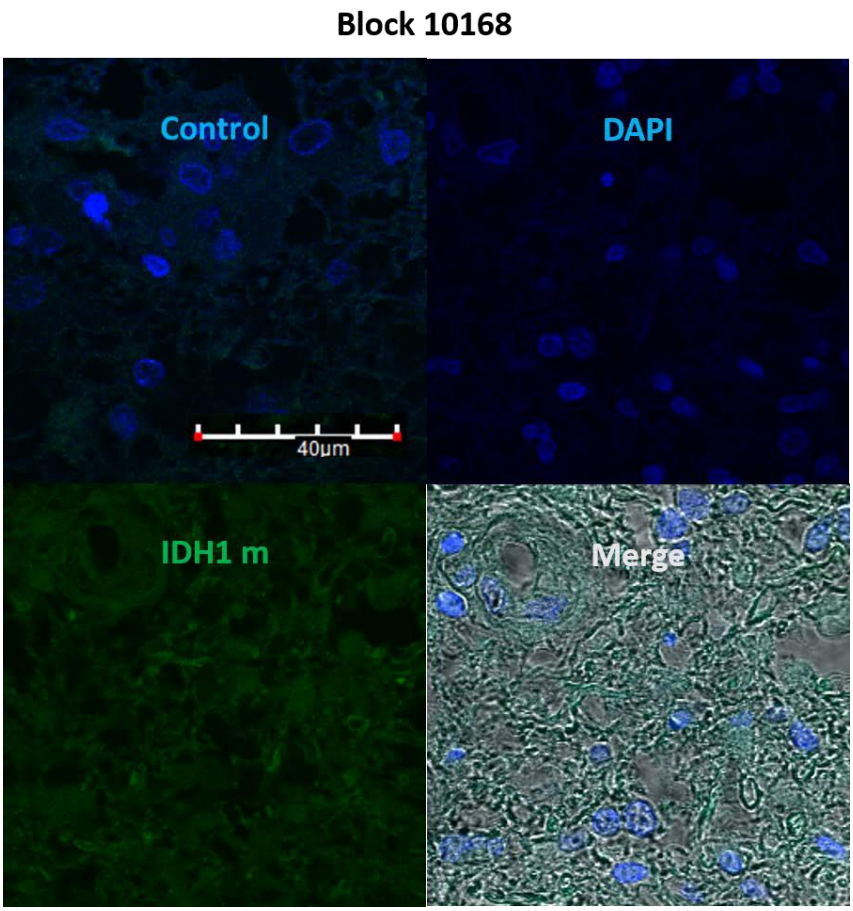

Figure 14C. **Immunofluorescence of IDH1 mutation in block 10168**. The control image is showing the absence of the secondary fluorescent antibody binding. The merged image is showing both DAPI staining and IDH1 mutation expression, along with the outlines of the cell bodies.

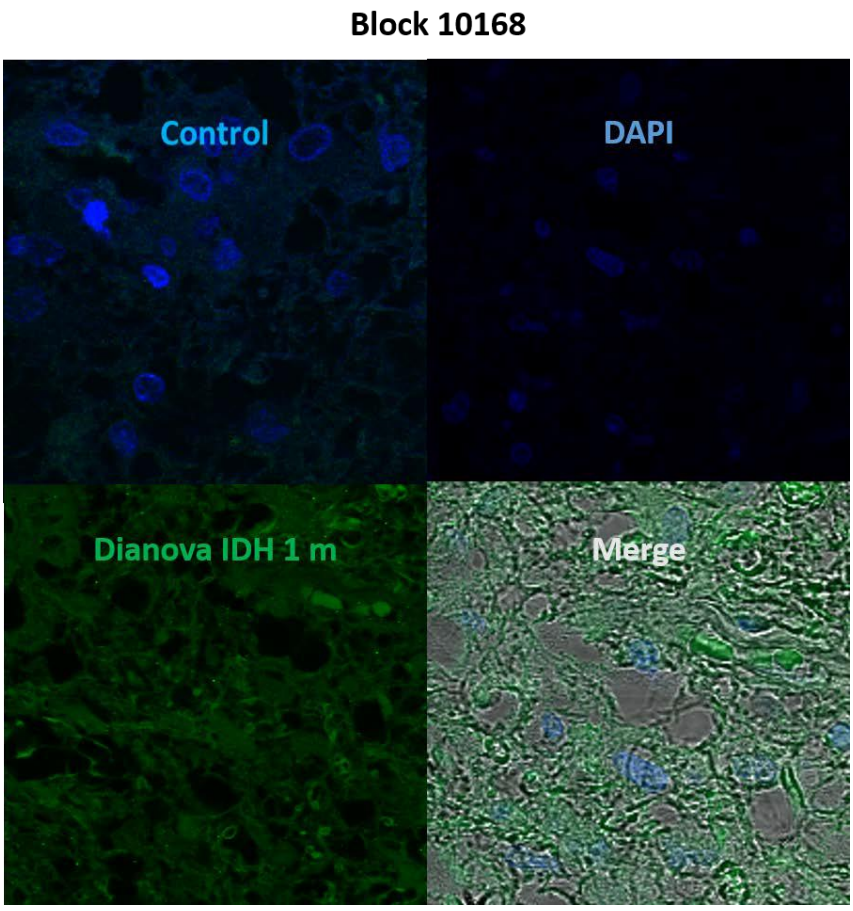

Figure 14D. Immunofluorescence of IDH1 mutation in block 10168. The control image is showing the absence of the Dianova fluorescent antibody binding. The merged image is showing both DAPI staining and IDH1 mutation expression, along with the outlines of the cell bodies.

Block 10168

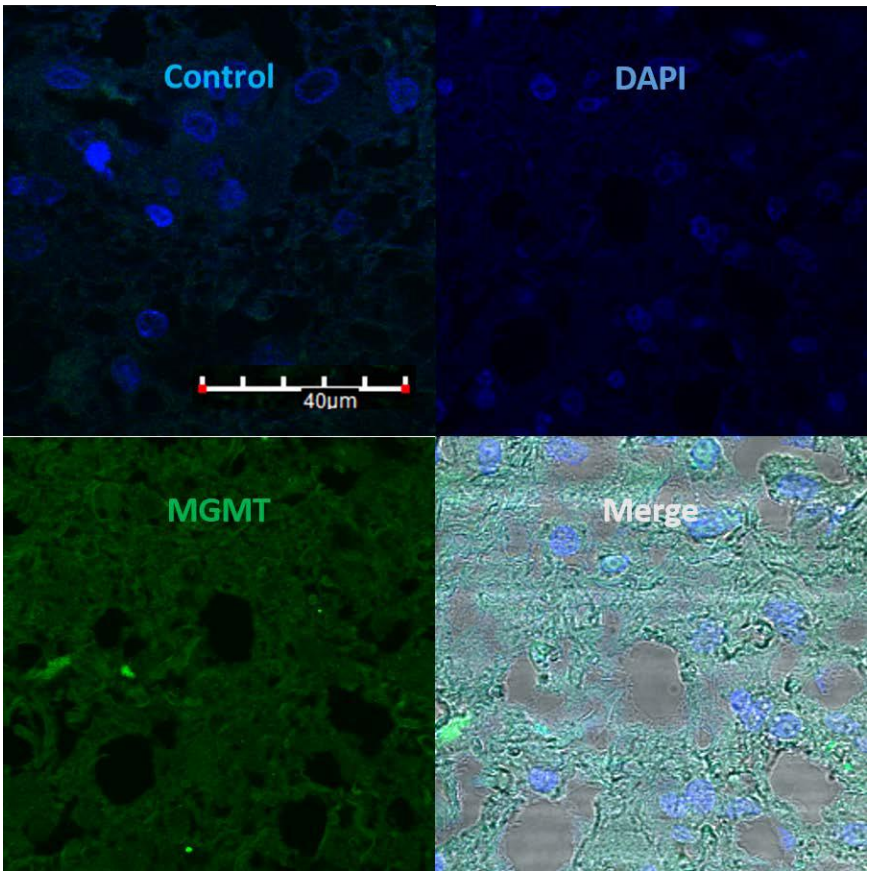

Figure 14E. **Immunofluorescence of MGMT in block 10168**. The control image is showing the absence of the secondary fluorescent antibody binding. The merged image is showing both DAPI staining and MGMT expression, along with the outlines of the cell bodies.

Block 8072

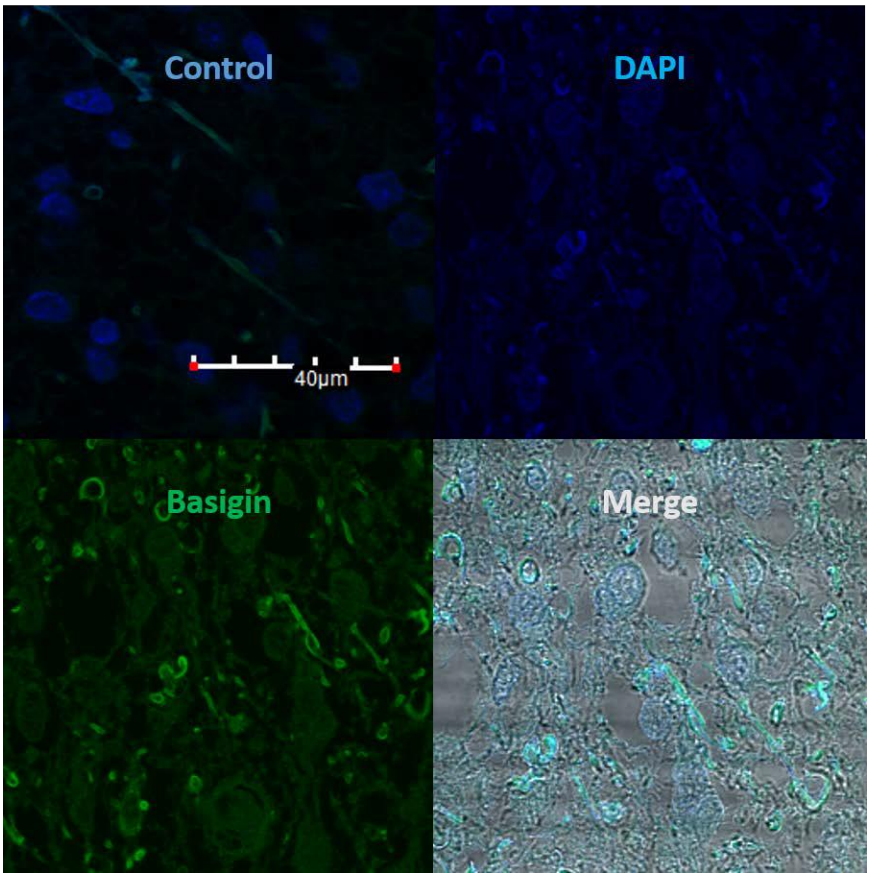

Figure 15A. **Immunofluorescence of Basigin in block 8072**. The control image is showing the absence of the secondary fluorescent antibody binding. The merged image is showing both DAPI staining and Basigin expression, along with the outlines of the cell bodies.

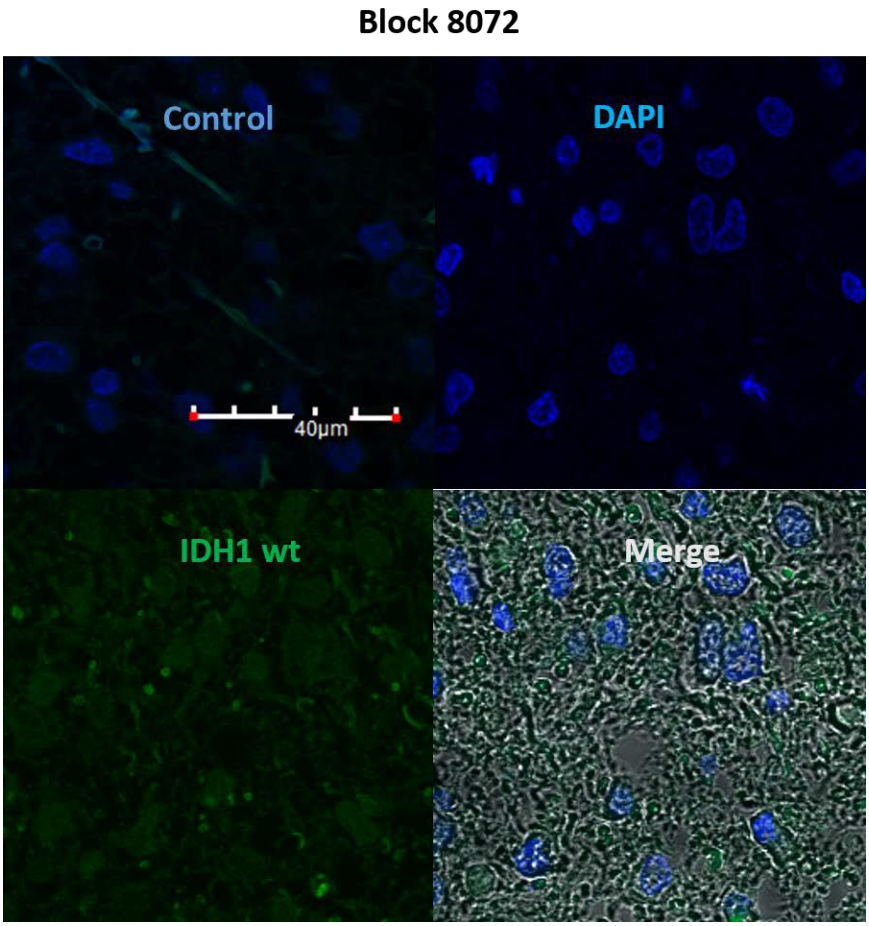

Figure 15B. Immunofluorescence of IDH1 wild type in block 8072. The control image is showing the absence of the secondary fluorescent antibody binding. The merged image is showing both DAPI staining and IDH1 wild type expression, along with the outlines of the cell bodies.

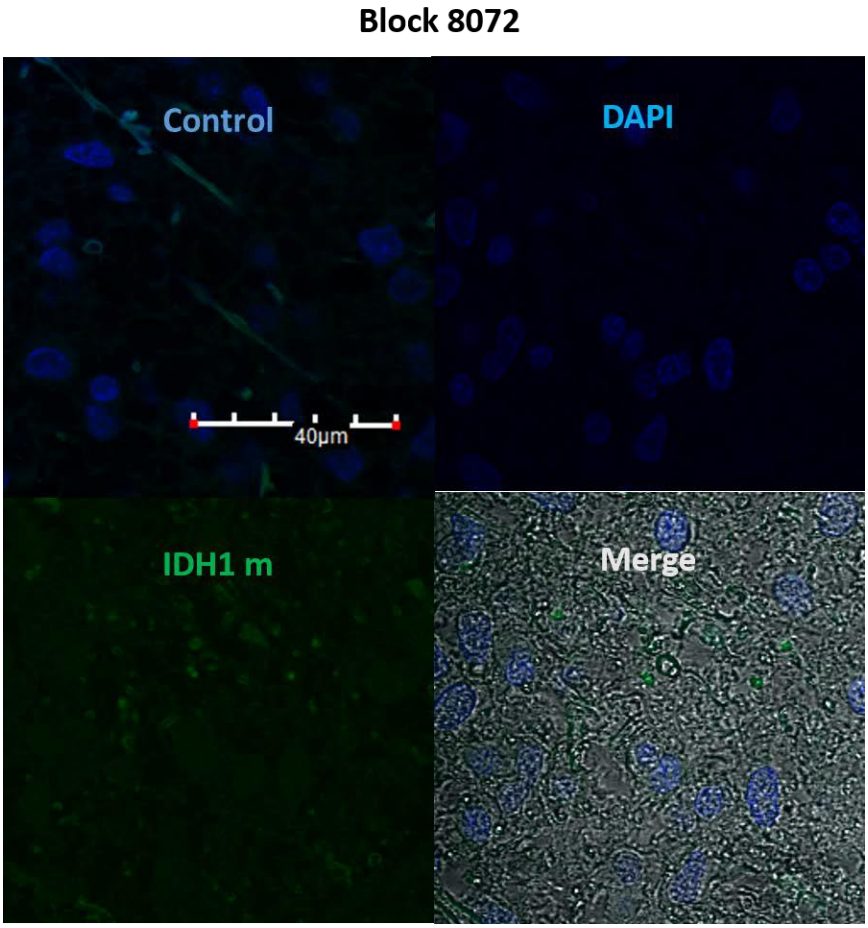

Figure 15C. **Immunofluorescence of IDH1 mutation in block 8072**. The control image is showing the absence of the secondary fluorescent antibody binding. The merged image is showing both DAPI staining and IDH1 mutation expression, along with the outlines of the cell bodies.

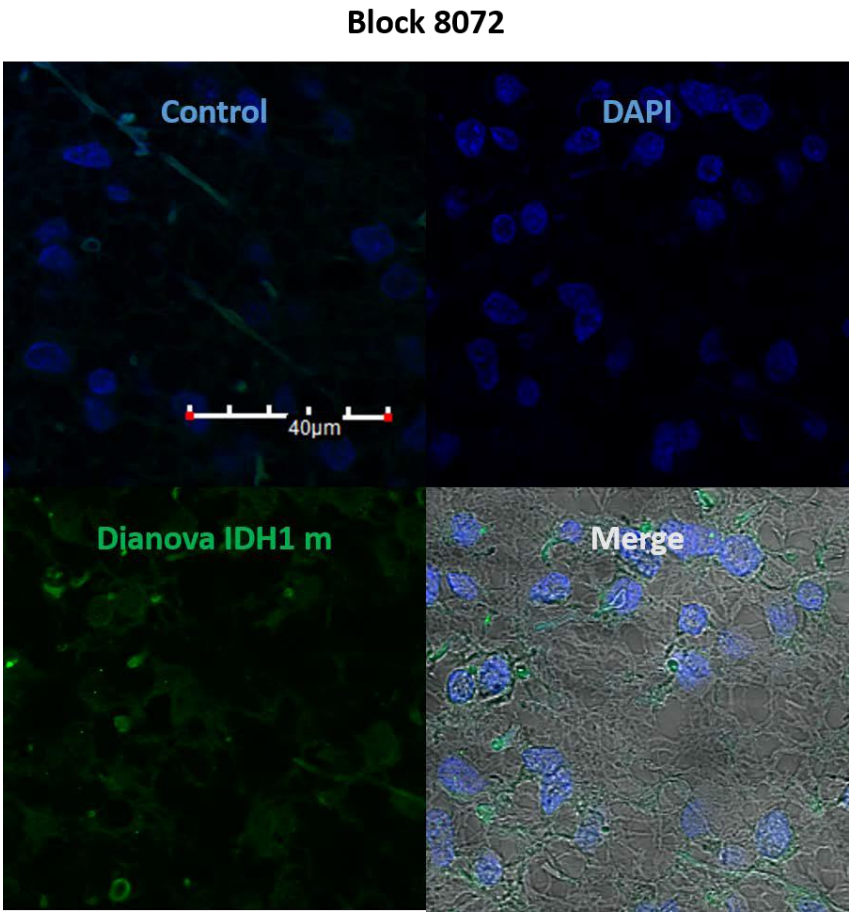

Figure 15D. **Immunofluorescence of IDH1 mutation in block 8072**. The control image is showing the absence of the Dianova fluorescent antibody binding. The merged image is showing both DAPI staining and IDH1 mutation expression, along with the outlines of the cell bodies.

Block 8072

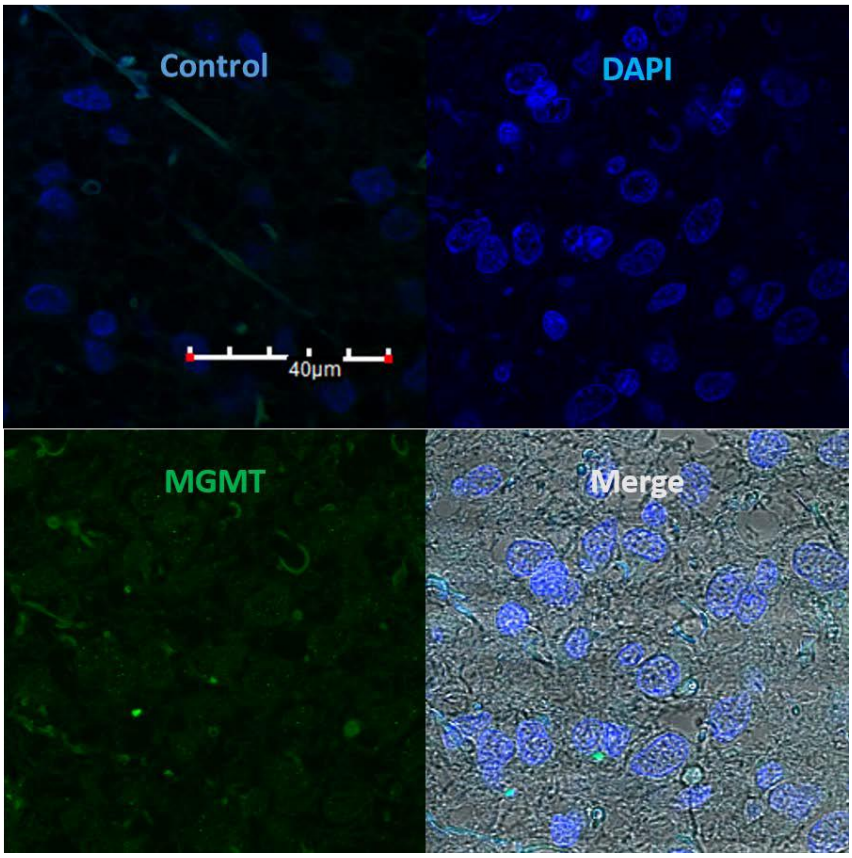

Figure 15E. **Immunofluorescence of MGMT in block 8072.** The control image is showing the absence of the secondary fluorescent antibody binding. The merged image is showing both DAPI staining and MGMT expression, along with the outlines of the cell bodies.

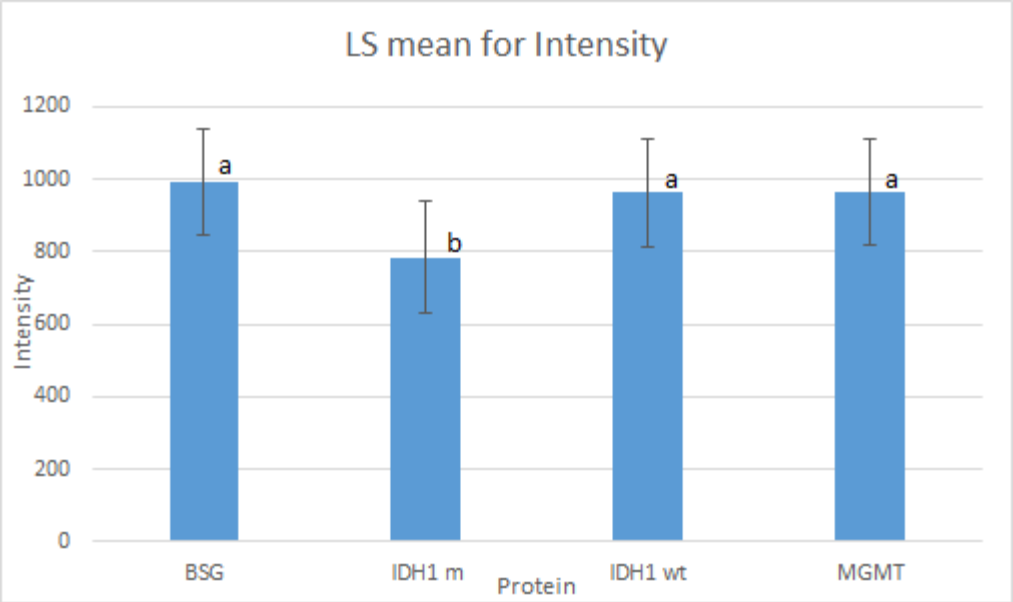

Figure 16A. Significant differences were found between the mean intensity of Basigin and IDH1 m (t ratio= 3.271, df= 493.80, P=0.006), IDH1m and IDHwt (t ratio=3.271, df=492.09, P=0.038), and IDH1m and MGMT (t ratio=2.830, df=492.15, P=0.025). No other pairs were found to be significantly different.

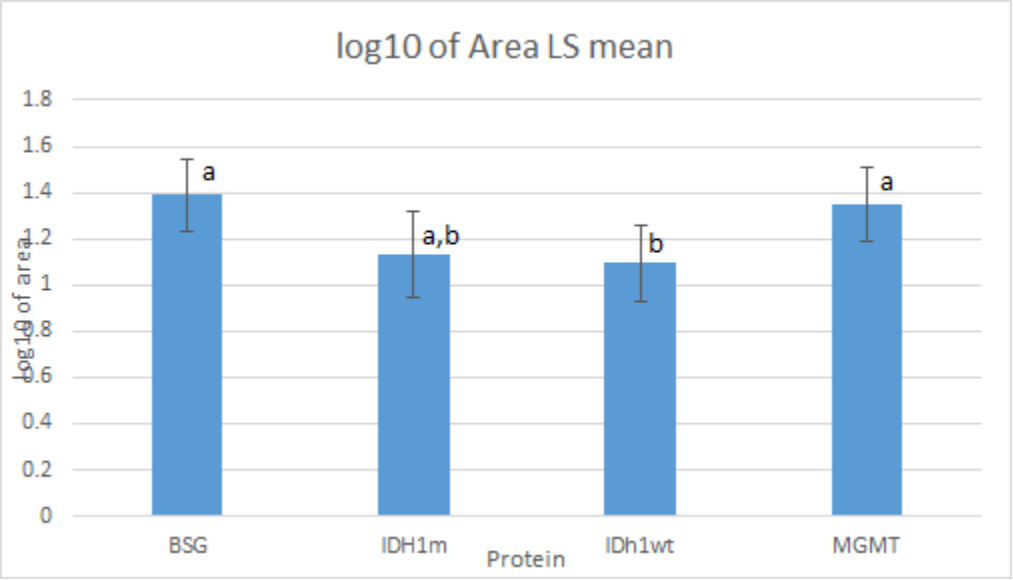

Figure 16B. Using the log 10 of area, significant differences were found between Basigin and IDH1 wt (P=0.006) and IDH1wt and MGMT (P=0.0188). Means with the same letter are not significantly different.

REFERENCES CITED

1. Holland EC. Glioblastoma multiforme: the terminator. *Proc Natl Acad Sci U S A*. 2000;97(12):6242-6244. http://www.pubmedcentral.nih.gov/articlerender.fcgi?artid=33993&tool=pmcentrez&rendertype=abstract. Accessed May 2, 2015.
2. Glioblastoma | American Brain Tumor Association. http://www.abta.org/brain-tumor-information/types-of-tumors/glioblastoma.html. Accessed October 16, 2014.
3. Parsons DW, Jones S, Zhang X, et al. An integrated genomic analysis of human glioblastoma multiforme. *Science*. 2008;321(5897):1807-1812. doi:10.1126/science.1164382.
4. Lawrence JE, Bammert C, Belton RJ, Rovin RA, Winn RJ. Targeting DNA Repair Mechanisms to Treat Glioblastoma. 2014:1-24.
5. Weinberg RA. The Biology of Cancer 2nd c2014.pdf. *2nd Ed*. 2014. http://www.scribd.com/doc/249762396/Weinberg-The-Biology-of-Cancer-2nd-c2014-pdf#scribd. Accessed March 14, 2016.
6. Knudson AG. Two genetic hits (more or less) to cancer. *Nat Rev Cancer*. 2001;1(2):157-162. doi:10.1038/35101031.
7. Singer E, Judkins J, Salomonis N, et al. Reactive oxygen species-mediated therapeutic response and resistance in glioblastoma. *Cell Death Dis*. 2015;6:e1601. doi:10.1038/cddis.2014.566.
8. Donnenberg VS, Donnenberg AD. Multiple drug resistance in cancer revisited: the cancer stem cell hypothesis. *J Clin Pharmacol*. 2005;45(8):872-877. doi:10.1177/0091270005276905.
9. Ohgaki H, Kleihues P. The definition of primary and secondary glioblastoma. *Clin Cancer Res*. 2013;19(4):764-772. doi:10.1158/1078-0432.CCR-12-3002.
10. Hanahan D, Weinberg RA. The Hallmarks of Cancer. *Cell*. 2000;100(1):57-70. doi:10.1016/S0092-8674(00)81683-9.
11. Cohen AL, Holmen SL, Colman H. IDH1 and IDH2 mutations in gliomas. *Curr Neurol Neurosci Rep*. 2013;13(5):345. doi:10.1007/s11910-013-0345-4.
12. Hamou M, Tribolet N De, Weller M, et al. MGMT Gene Silencing and Benefit from Temozolomide in Glioblastoma. 2005:997-1003.
13. Stupp R, Hegi ME, Mason WP, et al. Effects of radiotherapy with concomitant and adjuvant temozolomide versus radiotherapy alone on survival in glioblastoma in a randomised phase III study: 5-year analysis of the EORTC-NCIC trial. *Lancet Oncol*. 2009;10(5):459-466. doi:10.1016/S1470-2045(09)70025-7.
14. Ohgaki H, Dessen P, Jourde B, et al. Genetic pathways to glioblastoma: a population-based study. *Cancer Res*. 2004;64(19):6892-6899. doi:10.1158/0008-5472.CAN-04-1337.
15. Watanabe T, Nobusawa S, Kleihues P, Ohgaki H. IDH1 mutations are early events in the development of astrocytomas and oligodendrogliomas. *Am J Pathol*. 2009;174(4):1149-1153. doi:10.2353/ajpath.2009.080958.
16. Olivier M, Hollstein M, Hainaut P. TP53 mutations in human cancers: origins, consequences, and clinical use. *Cold Spring Harb Perspect Biol*. 2010;2(1):a001008.

doi:10.1101/cshperspect.a001008.
17. Miller CR, Perry A. Glioblastoma. October 2009. http://www.archivesofpathology.org/doi/full/10.1043/1543-2165(2007)131[397:G]2.0.CO;2. Accessed February 22, 2016.
18. Kloosterhof NK, Bralten LBC, Dubbink HJ, French PJ, van den Bent MJ. Isocitrate dehydrogenase-1 mutations: a fundamentally new understanding of diffuse glioma? *Lancet Oncol*. 2011;12(1):83-91. doi:10.1016/S1470-2045(10)70053-X.
19. 61207 - Clinical: IDH1/IDH2 Mutation Analysis by Pyrosequencing, Paraffin. http://www.mayomedicallaboratories.com/test-catalog/Clinical+and+Interpretive/61207. Accessed October 16, 2014.
20. van den Bent MJ, Dubbink HJ, Marie Y, et al. IDH1 and IDH2 mutations are prognostic but not predictive for outcome in anaplastic oligodendroglial tumors: a report of the European Organization for Research and Treatment of Cancer Brain Tumor Group. *Clin Cancer Res*. 2010;16(5):1597-1604. doi:10.1158/1078-0432.CCR-09-2902.
21. Turcan S, Rohle D, Goenka A, et al. IDH1 mutation is sufficient to establish the glioma hypermethylator phenotype. *Nature*. 2012;483(7390):479-483. doi:10.1038/nature10866.
22. Noushmehr H, Weisenberger DJ, Diefes K, et al. Identification of a CpG island methylator phenotype that defines a distinct subgroup of glioma. *Cancer Cell*. 2010;17(5):510-522. doi:10.1016/j.ccr.2010.03.017.
23. Weller M, Felsberg J, Hartmann C, et al. Molecular predictors of progression-free and overall survival in patients with newly diagnosed glioblastoma: a prospective translational study of the German Glioma Network. *J Clin Oncol*. 2009;27(34):5743-5750. doi:10.1200/JCO.2009.23.0805.
24. Kitange GJ, Carlson BL, Schroeder MA, et al. Induction of MGMT expression is associated with temozolomide resistance in glioblastoma xenografts. *Neuro Oncol*. 2009;11(3):281-291. doi:10.1215/15228517-2008-090.
25. Uno M, Oba-Shinjo SM, Camargo AA, et al. Correlation of MGMT promoter methylation status with gene and protein expression levels in glioblastoma. *Clinics*. 2011;66(10):1747-1755. doi:10.1590/S1807-59322011001000013.
26. Ishiguro K, Shyam K, Penketh PG, et al. Expression of O (6)-Methylguanine-DNA Methyltransferase Examined by Alkyl-Transfer Assays, Methylation-Specific PCR and Western Blots in Tumors and Matched Normal Tissue. *J Cancer Ther*. 2013;4(4):919-931. doi:10.4236/jct.2013.44103.
27. Becker K, Thomas AD, Kaina B. Does increase in DNA repair allow "tolerance-to-insult" in chemical carcinogenesis? Skin tumor experiments with MGMT-overexpressing mice. *Environ Mol Mutagen*. 2014;55(2):145-150. doi:10.1002/em.21834.
28. Muramatsu T, Miyauchi T. Basigin (CD147): a multifunctional transmembrane protein involved in reproduction, neural function, inflammation and tumor invasion. http://digitum.um.es/jspui/handle/10201/21468?mode=full&submit_simple=Show+full+item+record. Accessed October 16, 2014.
29. Bougatef F, Quemener C, Kellouche S, et al. EMMPRIN promotes angiogenesis through hypoxia-inducible factor-2alpha-mediated regulation of soluble VEGF isoforms and their receptor VEGFR-2. *Blood*. 2009;114(27):5547-5556. doi:10.1182/blood-2009-04-217380.
30. Biswas C, Zhang Y, DeCastro R, et al. The human tumor cell-derived collagenase

stimulatory factor (renamed EMMPRIN) is a member of the immunoglobulin superfamily. *Cancer Res*. 1995;55(2):434-439. http://www.ncbi.nlm.nih.gov/pubmed/7812975. Accessed April 16, 2015.
31. Raposo G, Stoorvogel W. Extracellular vesicles: exosomes, microvesicles, and friends. *J Cell Biol*. 2013;200(4):373-383. doi:10.1083/jcb.201211138.
32. Sidhu SS, Mengistab AT, Tauscher AN, LaVail J, Basbaum C. The microvesicle as a vehicle for EMMPRIN in tumor-stromal interactions. *Oncogene*. 2004;23(4):956-963. doi:10.1038/sj.onc.1207070.
33. Belton RJ, Chen L, Mesquita FS, Nowak R a. Basigin-2 is a cell surface receptor for soluble basigin ligand. *J Biol Chem*. 2008;283(26):17805-17814. doi:10.1074/jbc.M801876200.
34. Yang M, Yuan Y, Zhang H, et al. Prognostic significance of CD147 in patients with glioblastoma. *J Neurooncol*. 2013;115(1):19-26. doi:10.1007/s11060-013-1207-2.
35. R: a language and environment for statistical computing | GBIF.ORG. http://www.gbif.org/resource/81287. Accessed March 17, 2016.
36. Bates D, Mächler M, Bolker B, Walker S. Fitting Linear Mixed-Effects Models Using lme4. *J Stat Softw*. 2015;67(1):1-48. doi:10.18637/jss.v067.i01.
37. Liang Q, Xiong H, Gao G, et al. Inhibition of basigin expression in glioblastoma cell line via antisense RNA reduces tumor cell invasion and angiogenesis. *Cancer Biol Ther*. 2014;4(7):759-762. doi:10.4161/cbt.4.7.1828.
38. Dimitrov L, Hong CS, Yang C, Zhuang Z, Heiss JD. New developments in the pathogenesis and therapeutic targeting of the IDH1 mutation in glioma. *Int J Med Sci*. 2015;12(3):201-213. doi:10.7150/ijms.11047.
39. Li S, Chou A, Chen W, Chen R, Deng Y, Phillips H, Selfridge J, Zurayk M, Lou J, Everson R, Wu K, Faull K, Cloughesy T, Liau L, Lai A. Overexpression of isocitrate dehydrogenase mutant proteins renders glioma cells more sensitive to radiation. *Neuro-Oncology* 2013;15(1):57–68. doi:10.1093/neuonc/nos261
40. Thon N, Kreth S, Kreth F. Personalized treatment strategies in glioblastoma: *MGMT* promoter methylation status. *OncoTargets and Therapy* 2013;6:1363-1372